MAXFAS:

A MOBILE ARM EXOSKELETON FOR FIREARM AIM STABILIZATION

by

Daniel M. Baechle

A thesis submitted to the Faculty of the University of Delaware in partial fulfillment of the requirements for the degree of Master of Science in Mechanical Engineering

Spring 2013

MAXFAS:

A MOBILE ARM EXOSKELETON FOR FIREARM AIM STABILIZATION

by

Daniel M. Baechle

Approved: _____
Sunil K. Agrawal, Ph.D.
Professor in charge of thesis on behalf of the Advisory Committee

Approved: _____
Suresh G. Advani, Ph.D.
Chair of the Department of Mechanical Engineering

Approved: _____
Babatunde A. Ogunnaike, Ph.D.
Dean of the College of Engineering

Approved: _____
James G. Richards, Ph.D.
Vice Provost for Graduate and Professional Education

ACKNOWLEDGMENTS

I would like to express my gratitude to my advisor Dr. Sunil K. Agrawal for his patience and expertise offered in helping me complete this project. His advice was invaluable in helping me solve the robotics problems involved in this thesis, a field which was entirely new to me when I started this project. He had faith in me at times when I did not have faith in myself.

I would also like to thank my committee members, Dr. Ioannis Poulakakis and Dr. Herbert Tanner for examining my thesis dissertation and providing their insights during my dissertation defense.

I offer my sincere thanks to my team leader Eric Wetzel at the U.S. Army Research Laboratory. His original ideas have motivated my work efforts throughout the years, and his application of technical expertise to the benefit of the soldier provides the inspiration I use in shaping my current and future career.

I cannot thank Dr. Ying Mao enough for his assistance throughout this project. Without his advice, I could not have completed this project. Dr. Mao had nearly completed his Ph. D when I was starting my thesis. He had no obligation to help me after completing his Ph. D and starting a job far away, but continued to offer advice whenever I asked.

Many of the students in the Mechanical Systems Laboratory assisted my efforts and experiments, and I would be remiss not to thank them. In particular, I would like to thank Xin Jin, Damiano Zanotto, Vineet Vashista, Paul Stegall, Joon Park and Shazlin Sharaudin for their exemplary help.

Through decades of example, my parents Daniel A. Baechle and Kathryn A. Murphy taught me the strong work ethic I required to complete my classes and thesis. Indeed, without their encouragement, teachings, and support, I would not be in the position I am in now. I will always be grateful for all they have done for me.

And finally, I cannot thank my beautiful wife Christy Clark Baechle enough. We were dating when I began my studies for this degree. Her patience and devotion through my long nights and absent days helped me realize that she was indeed the one with whom I should spend the rest of my life. My greatest reward is the extra time I will have to spend with my love, my life, my wife Christy.

TABLE OF CONTENTS

LIST OF TABLES

LIST OF FIGURES

ABSTRACT

Accurately aiming and firing a pistol requires a steady hand. While many devices can steady a shooter's arm or hand by restricting movement or degrees of freedom, few devices actively reduce involuntary tremors while allowing larger voluntary aiming movements. This paper details the design, fabrication, and experimental evaluation of an arm exoskeleton that can actively damp arm tremors while allowing voluntary aiming movements. The MAXFAS (Mobile Arm eXoskeleton for Firearm Aim Stabilization) device allows five degrees of freedom, controlling four degrees of freedom using thin steel cables. The cable-driven architecture allows the control motors to be mounted away from the arm, resulting in device that adds very little weight and inertia to the arm. The cables attach to braces that are mounted on the forearm and upper arm. Weight of MAXFAS is further reduced compared to conventional arm exoskeletons through the careful design and manufacture of the braces using stiff, lightweight carbon fiber composites. The initial design called for tremorous movement to be filtered out from voluntary motion, and an adaptive algorithm to provide a tremor-cancelling signal to the cable control motors. Experiments described in this paper involved a control method which used the motors to only actively allow voluntary motion, thus attempting to passively damp tremorous motion. The device was evaluated on subjects performing a pistol aiming task, using an airsoft pistol with a laser sight. Results indicate that this simpler control mode was effective at reducing the amplitude of motion in all five degrees of freedom. During a simulated shooting task, this control mode improved shooting performance

both while subjects were wearing the device, as well as 5 minutes after removing the device. These results will be discussed, and future experiments will be suggested.

Chapter 1

INTRODUCTION

1.1 Background: Exoskeletons

Over the past 40 years, extensive research has taken robotic exoskeletons from realm of science fiction to reality. The concept is simple – a wearable device that can aid human performance, be it strength, speed or agility. However, early robotic technology was insufficient to make such a device feasible for real-world use. Early devices such as GE's Hardiman (Figure 1), though designed to aid human performance, were enormous, heavy, and inefficient [1]. Advances in computer control, structural materials science, energy storage batteries and actuation technologies have allowed exoskeletons to dramatically shrink in size while improving effectiveness.

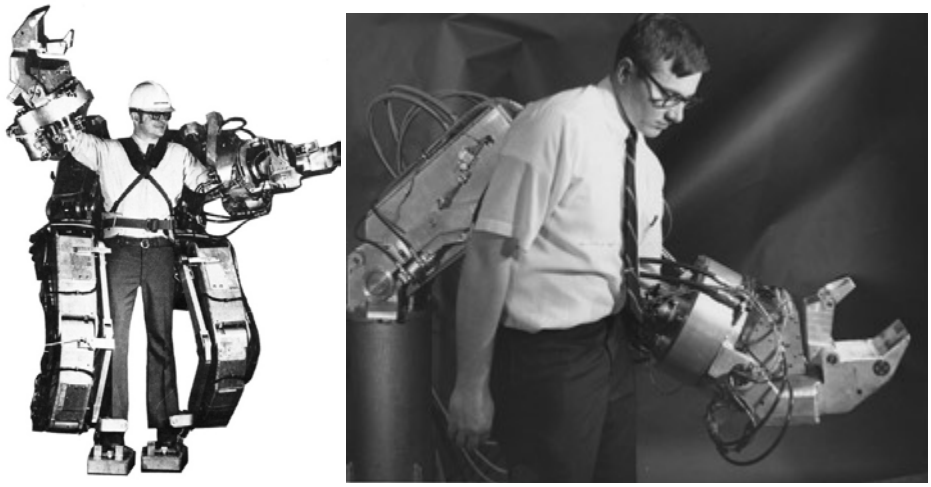

Figure 1: GE's Hardiman exoskeleton, c. 1968 [1].

Raytheon's full-body XOS 2 (Figure 2) weighs 195 lbs and increases the wearer's strength by a factor of 17, allowing a person to lift loads that would otherwise be difficult or impossible unaided [2]. The XOS 2 is a tethered device, with hydraulic power supplied by cables running to equipment that must remain nearby. Lockheed Martin's HULC device (Figure 3), which has evolved from work at Berkley's exoskeleton group, is an untethered leg exoskeleton consisting of rigid titanium links with joints at the hip, knee and ankle [3]. Hydraulics provide power assistance at the hip and knee joints. The device allows the wearer to carry up to 200 lb loads for 20 km on a single battery charge, transferring the load from the back to the ground through the titanium links. The HULC device is currently being field-tested by the U.S. Army to determine if the device improves metabolic efficiency of the wearer [4].

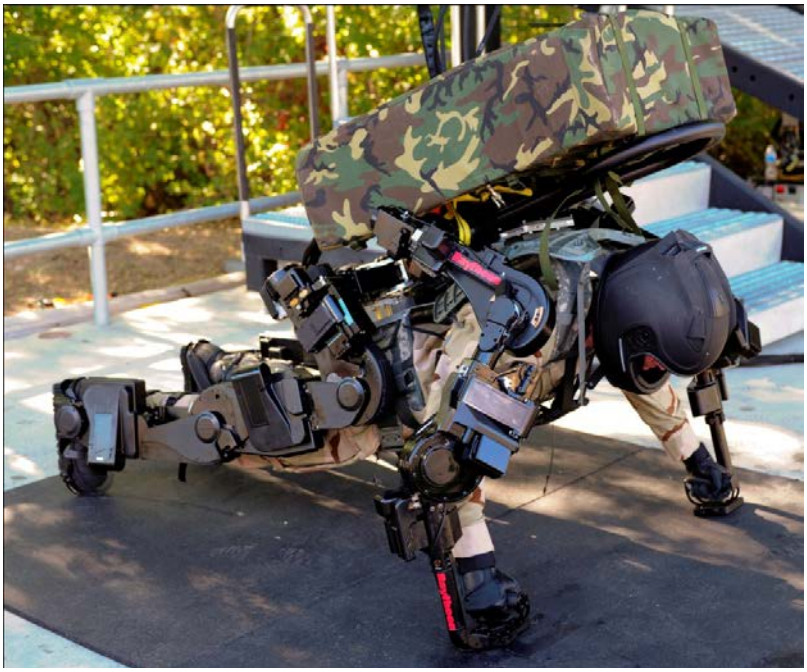

Figure 2: Raytheon's XOS 2 [5]

Figure 3: Lockheed Martin's HULC [3]

Exoskeletons have also proven useful tools for human rehabilitation. Rather than only increasing performance while the user is wearing the device, exoskeletons can be used to re-train disabled people to properly use their appendages. The ALEX and ALEX II devices at the University of Delaware's Mechanical Systems Laboratory are tethered leg exoskeletons for rehabilitation of stroke victims (Figure 4) [6], [7], [8]. The devices use an assist-as-needed control paradigm. A computer creates a desired gait path for the wearer. If the wearer's leg moves perfectly along the desired path, the ALEX device applies no force to the leg. However, if the wearer's leg strays from the desired path, the device applies a force to guide the leg onto the desired path. The amount of applied force is governed by a virtual "force tunnel" around the desired path. Studies using the ALEX device have shown that the device and control method are effective at modifying the gait of healthy subjects and stroke patients after training in the devices [6] [7].

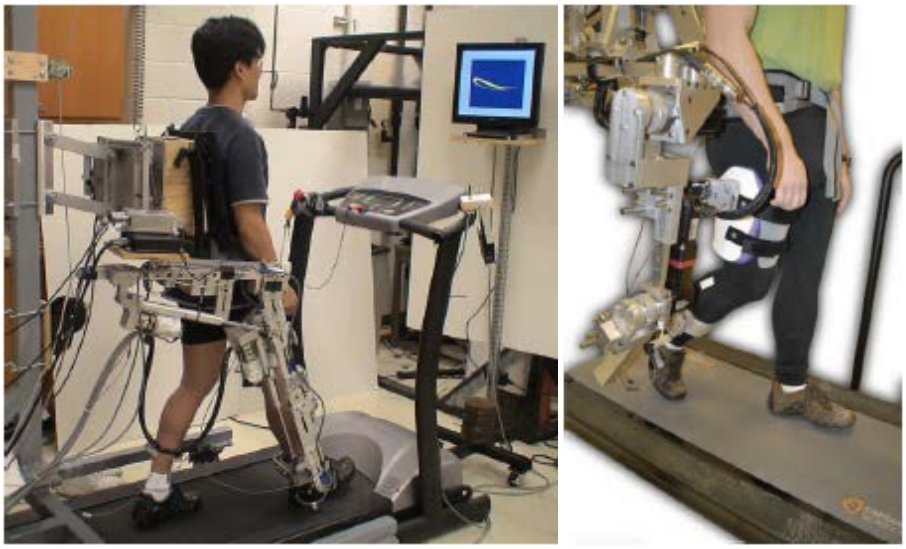

Figure 4: University of Delaware's ALEX (left) and ALEX II (right) devices [7], [8]

The University of Delaware group has also developed a cable-driven arm exoskeleton for rehabilitation purposes. The CAREX device uses a similar assist-as-needed control method, using a virtual force tunnel to guide the wearer's arm along a path for a predetermined task (Figure 5) [9]. Training with the CAREX device has been shown to improve a healthy subject's ability to follow an invisible path, even after the force control is turned off. Critically, the mass of extra equipment on the arm is only 1.32 kg, approximately an order of magnitude lower mass on the arm than other arm exoskeletons for rehabilitation. These devices include BONES [10], CADEN-7 [11], SAM [12], and RUPERT [13], seen in Figure 6 and Figure 7. These rigid exoskeletons can compensate for the extra static weight on the arm using motors, but the added inertia of the device caused by arm motion cannot be compensated. Additionally, rigid-link exoskeletons require precise joint alignment for optimal performance. Even with proper alignment, the rigid exoskeleton can cause discomfort for the wearer. Unlike typical robotic joints, arm joints do not rotate perfectly about

one stationary point [14]. The rigid exoskeleton can be aligned to the arm joints in one position, but the arm joint centers can become misaligned with the robot joints during arm movement. Such misalignment can lead to poor performance, discomfort and even skin sores for the wearer.

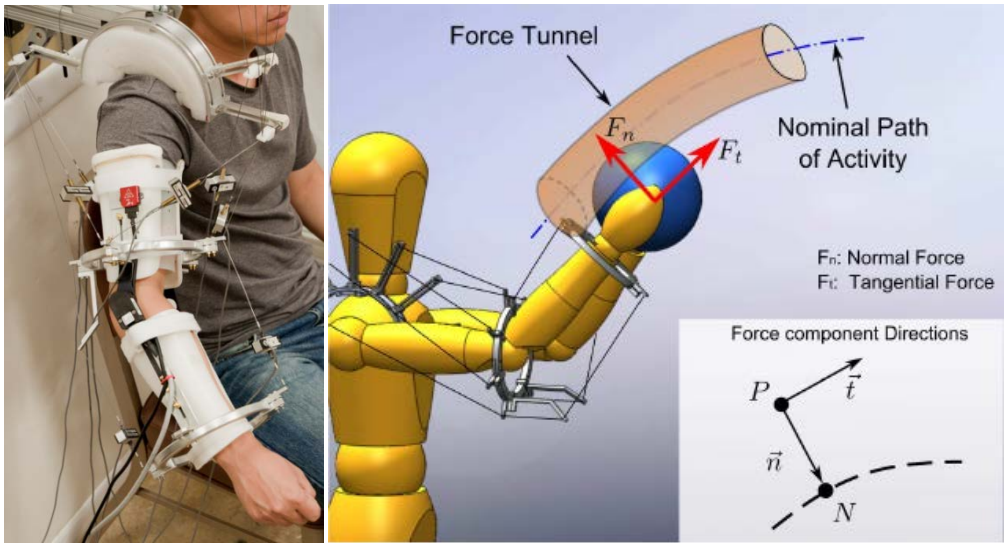

Figure 5: University of Delaware's CAREX [9]

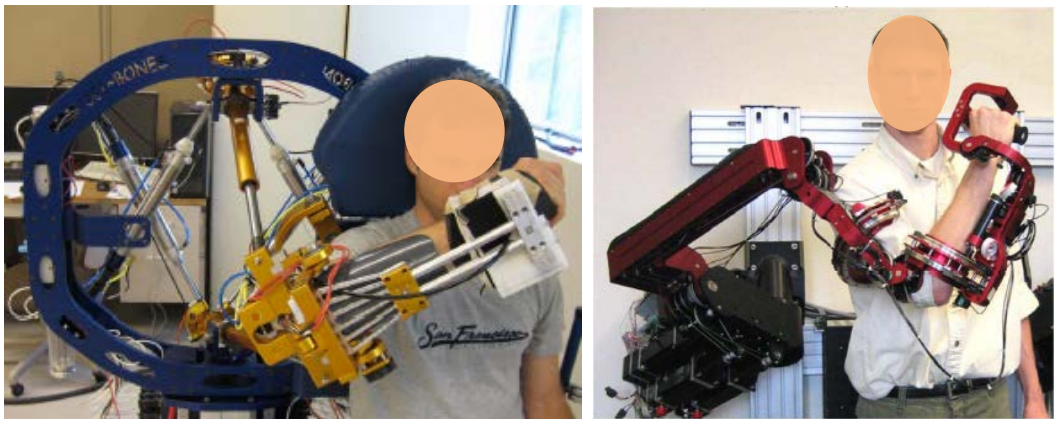

Figure 6: BONES [10] (left) and CADEN-7 [11] (right)

Figure 7: SAM [12] (left) and RUPERT [13] (right)

Rocon and Pons have developed an arm exoskeleton specifically for suppression of pathological tremors in the upper arm [15]. Their WOTAS device consists of DC motors mounted on a rigid orthotic structure on the arm, providing control of 3 degrees-of-freedom (DOF) at the elbow and wrist (Figure 8). Though the device has rigid links and motors mounted directly on the arm, it adds only 850 g to the arm. MEMS gyroscopes mounted on the arm measure tremorous movement in the wearer's arm. A computer algorithm separates tremorous movement from voluntary movement in the gyroscope signal, and estimates the frequency of the tremor. The DC motors then create anti-phase movement in the arm in order to cancel the measured tremor. Results of a small trial found the WOTAS device able to reduce tremor power by an average of 40% for wearers with essential Parkinsonian and other pathological tremor.

Figure 8: WOTAS device [15]

1.2 Aim Stabilization

Tremors in the arm, whether pathological or postural (due to holding the arm outstretched), have also been shown to negatively affect aiming tasks [16], [17], [18]. However, accuracy when aiming and shooting a firearm depends on many factors. These factors can be divided into three primary groups: environmental, hardware, and human factors. Numerous devices exist to mitigate the negative influence of environmental factors such as available light, ambient noise, and wind. Hardware has been made as accurate as possible using special barrels, ammunition, scopes and laser sights. However, even the most accurate firearm in an ideal environment is subject to the human factors that affect aim, which include fatigue [19], heart rate [20], shooting experience [21], body sway [22], and arm tremors. Some static devices attempt to stabilize the arm and reduce tremors by reducing range of motion or degrees of freedom [23]. Other devices attempt to reduce arm tremors using passive elements such as springs or dampers [24]. A 1991 US patent describes a device that is

essentially a gyroscope mounted to the back of the hand, intended to reduce tremors in the hand [25]. Similarly, a rifle-mounted gyroscope to reduce small aiming errors was awarded a US patent in 1992 [26]. Tactical Electronics currently offers a gyroscopically stabilized rifle platform for the same purpose [27]. However, none of these devices actively sense and cancel arm tremors, as in the WOTAS device.

1.3 MAXFAS: Mobile Arm eXoskeleton for Firearm Aim Stabilization

The device described in this work is a wearable arm exoskeleton which senses and cancels tremorous motion in the arm of the wearer during an aiming and firing task. Similar in functionality to the WOTAS device, adaptive filters separate tremorous movement, allowing larger voluntary movements necessary for aiming. The mobile arm exoskeleton for firearm aim stabilization (MAXFAS) device of this paper is novel in several key ways. The MAXFAS device is cable-driven: motors are not mounted on the arm, but above or behind the user. The cable-driven design allows for a lighter exoskeleton, adding less than 280 g to the wearer's arm. Carbon fiber composite materials also make MAXFAS very low-weight, while maintaining the structural rigidity required to control the arm. The MAXFAS device is an evolution of the CAREX device. Unlike CAREX and WOTAS however, MAXFAS has no rigid joint at the elbow, eliminating joint alignment issues. The MAXFAS device consists of braces attached to the forearm and upper arm. MAXFAS allows five DOF: flexion/extension, adduction/abduction, internal/external rotation of the shoulder, flexion/extension of the elbow, and pronation/supination of the forearm. The device is designed such that forearm rotation is somewhat constrained to minimize rotation away from the desired aiming position. The wrist and hand are not controlled. A preliminary experiment without the MAXFAS device was first performed to

determine the sensing requirements of the device, and if wrist control was necessary. This preliminary experiment will be described in the following chapter. Design of the MAXFAS device, control system, and adaptive filter is described in later chapters, along with the design and results of human experiments.

Chapter 2

PRELIMINARY AIMING EXPERIMENT

2.1 Experiment

Prior to designing the MAXFAS device, an experiment was performed to evaluate key equipment and parameters to be used in the MAXFAS experiments. The MAXFAS device required a sensor accurate enough to detect tremors in the arm. Additionally, the MAXFAS experiments involved the subject aiming a toy pistol at a target, and thus required the ability to track the subject's aim point on the target. The preliminary experiment tested a VN-100r inertial measurement unit (IMU) from Vectornav Technologies, LLC. The VN-100r incorporates a 3-axis accelerometer, 3-axis gyroscope, and 3-axis magnetometer. The VN-100r also uses an on-board processor to filter and compensate for drift in real-time. The VN-100r measures 36×33×9 mm, and weighs only 13 g (not including power/data cable). For the preliminary experiment, the VN-100r was attached to the handle of a toy pistol, as seen in Figure 9. The barrel of the pistol was replaced with a 780 nm wavelength IR laser. A visible red laser was mounted underneath the barrel, as seen in Figure 9. A Vicon Bonita motion capture system, which operates at 780 nm, was used to track the IR laser on a 30×30 cm white target with black crosshairs, seen in Figure 10.

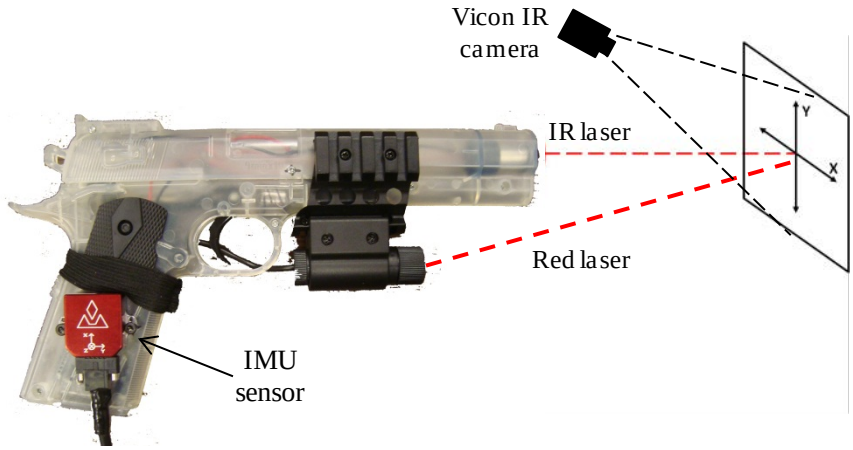

Figure 9: Device for preliminary experiments

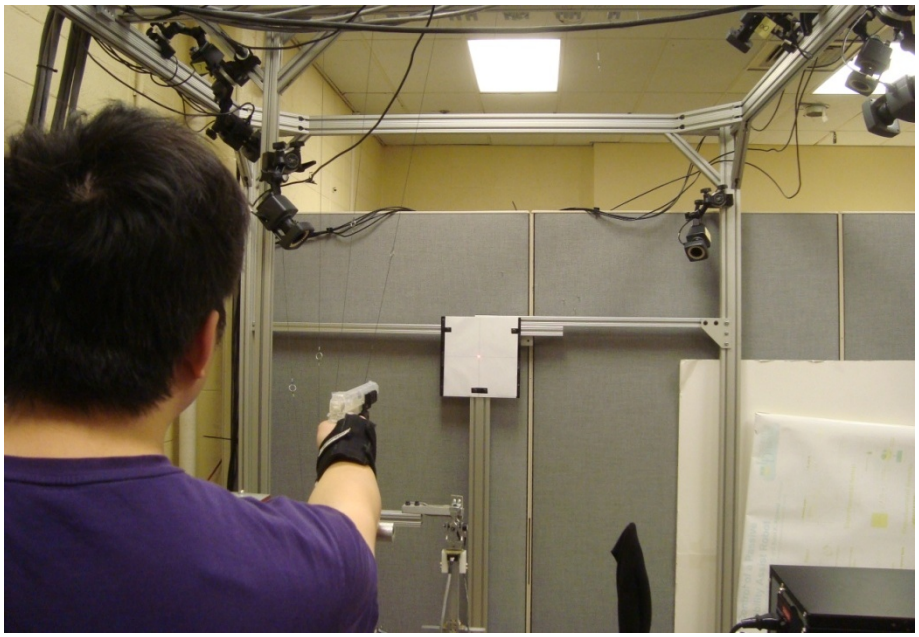

Figure 10: Subject during preliminary experiment

Each subject was instructed to hold the toy pistol and aim the red laser at the target (approximately 2.5 meters from the subject) for 30 seconds in 7 different

scenarios. The scenarios are enumerated in Table 1, and were designed to test the effect of static arm and wrist stabilization and constraint on arm tremor and aim. A simple wrist brace was used to constrain the dominant wrist in scenarios 2, 3 and 6. Subjects wrested the forearm of their dominant arm on a 140 cm tall stand in scenarios 5 and 6.

Table 1: Preliminary experiment scenarios

Scenario	Arms	Wrist Brace	Arm Stand
1	1	N	N
2	1	Y	N
3	2	N	N
4	2	Y	N
5	1	N	Y
6	1	Y	Y

Ten right-handed subjects were tested: 9 males and 1 female. Only one subject had any shooting experience. Figure 11 presents the standard deviation of the IR laser x- and y-positions, averaged across all 10 subjects. As the experiment is primarily concerned with differences in tremors between the scenarios, only standard deviation of the aim point is presented. Accelerometer and gyroscope data from the VN-100r was recorded to directly measure the subjects' arm tremors. A representative plot of IR laser x-position vs. time for a single subject in trials 1 and 5 can be seen in Figure 12. A representative plot of accelerometer data vs. time for a single subject in trials 1 and 5 can be seen in Figure 13. A representative plot of gyroscope data vs. time for a

single subject in trials 1 and 5 can be seen in Figure 14. Figure 12 illustrates the static signal recorded by the Vicon system while the laser sat motionless and untouched, indicating that the Vicon system can record the laser point with sub-millimeter accuracy. Figure 13 and Figure 14 also illustrate the static signal from the accelerometer and gyroscope, respectively, which was recorded while the VN-100r sat motionless and untouched.

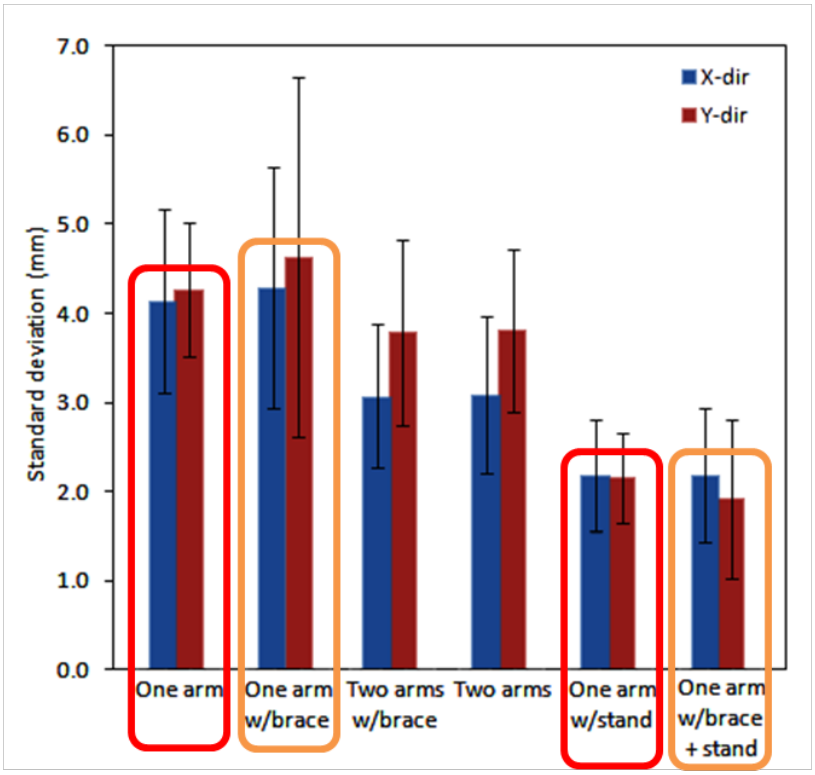

Figure 11: Average standard deviation of laser point

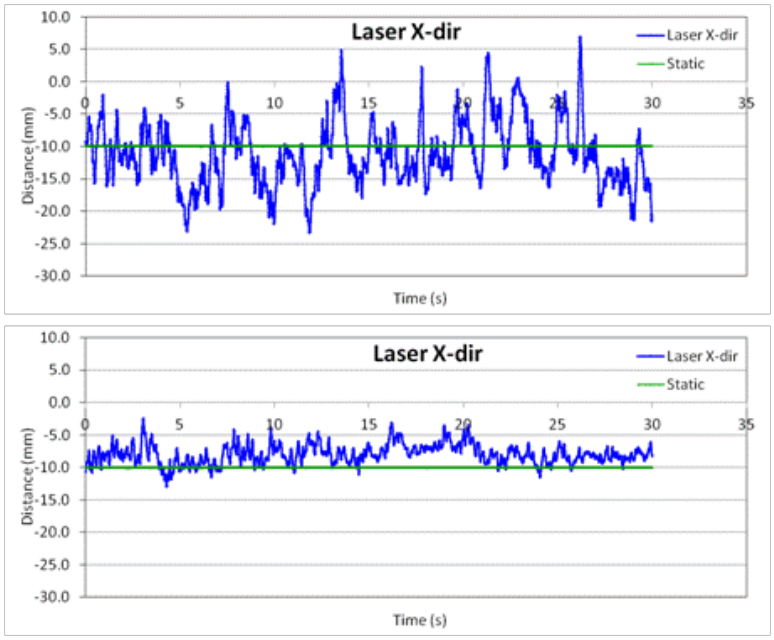

Figure 12: IR laser x-position for representative subject, scenarios 1 (top) and 5 (bottom)

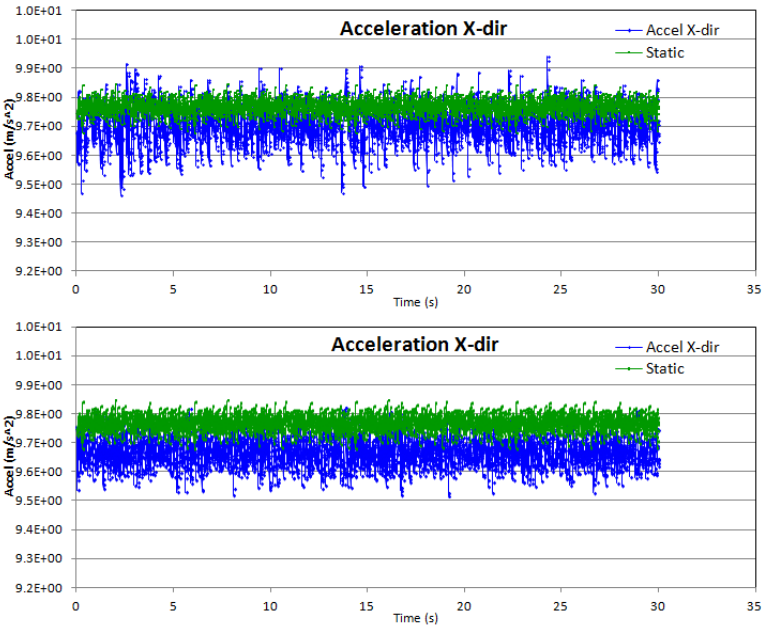

Figure 13: Accelerometer data for representative subject, scenarios 1 (top) and 5 (bottom)

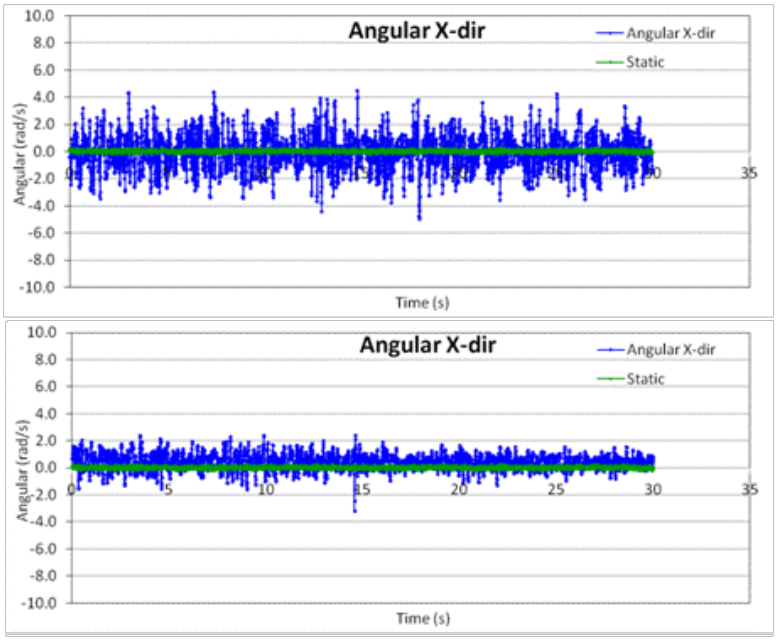

Figure 14: Gyroscope data for representative subject, scenarios 1 (top) and 5 (bottom)

2.2 Discussion & Conclusions

Comparing scenarios 1 to 2 and 5 to 6 in Figure 11, it is evident that the standard deviation of the IR laser aim point did not significantly decrease when the subjects were wearing the wrist brace. This result indicates that wrist control is not a critical factor in improving aim, and will not be necessary in the MAXFAS device. Comparing scenarios 1 to 5 and 2 to 6 in Figure 11, it is evident that the standard deviation of the IR laser aim point significantly decreased when the subjects rested their dominant arm on the stand. This result can also be seen in Figure 12. This result indicates that a device that can steady the arm during aiming will significantly improve aim. The accelerometer data in Figure 13 indicates that the accelerometers in the VN-100r are not sensitive enough to detect significant changes in arm tremor. However, the gyroscope data in Figure 14 indicates that the gyroscopes are sensitive

enough to detect significant changes in arm tremor. As such, the gyroscopes on the VN-100r will be used to track arm tremors in the MAXFAS device.

Chapter 3

MAXFAS

3.1 Introduction

MAXFAS is a unique arm exoskeleton designed specifically to improve aim while adding little mass and volume to the arm. The basic concept of a cable-driven arm exoskeleton was adapted from the CAREX device. However, whereas CAREX used force control to guide the arm along a specified path in space, MAXFAS was designed to allow a wider variety of large movements of the arm while actively damping only the small tremors in the arm. This chapter details the design and fabrication of the MAXFAS device, considering the functional requirements and physical constraints.

3.2 Design and System

3.2.1 Exoskeleton Design

An illustration of the MAXFAS device can be seen in Figure 15. The exoskeleton consists of three braces: one on the anterior (inner) forearm, and one each on the inner and outer upper arm. Six cables are used to control the arm: two cables terminating at each brace. Thus, four cables govern the flexion/extension, adduction/abduction, and internal/external rotation of the upper arm. Two cables terminating on the forearm brace near the wrist govern flexion/extension of the forearm. These two cables are routed through the outer upper arm brace, near the

elbow. Note that although forearm pronation/supination cannot be explicitly controlled in this configuration, the location of the cable termination points on the forearm brace and routing points of these cables on the upper arm brace constrain rotation away from the proper aiming position when the cables are tensioned. Additionally, the forearm brace itself constrains forearm rotation away from the proper aiming position. Cable termination and routing points were chosen based on the CAREX design.

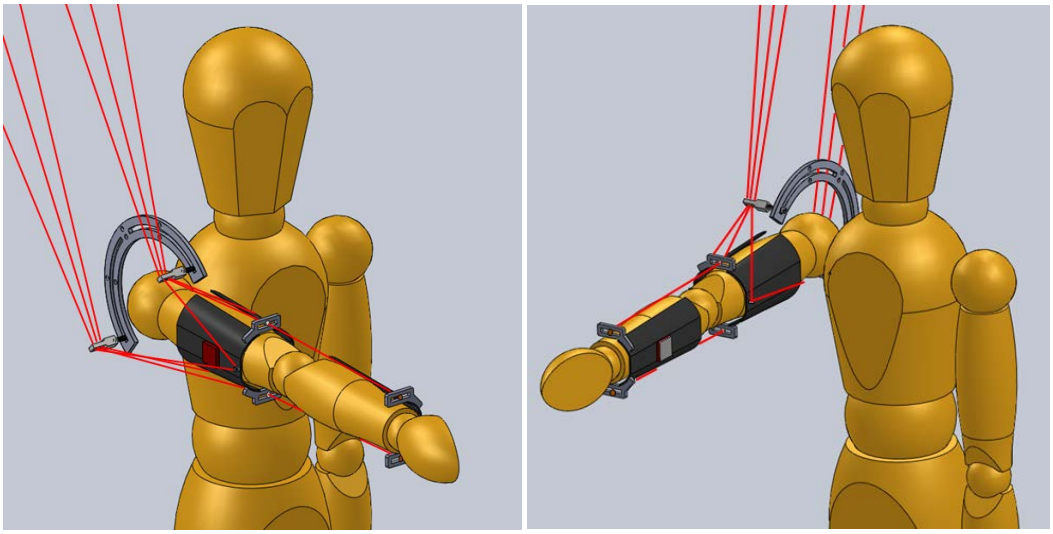

Figure 15: An illustration of MAXFAS, cables shown in red for clarity

3.2.2 Composite Braces

Each brace consists of a 1 mm thick carbon fiber laminate shell, custom manufactured to minimize weight while providing the structural stiffness necessary to transmit control to the arm using cables. The shell consists of 8 plies of carbon fiber prepreg (Cytec Cycom IM7-381). Each ply is unidirectional, having carbon fibers running in only one direction. Ply orientation design analysis was performed using a custom program in MATLAB. The program uses the principles of classical laminate theory to determine the mechanical properties of any sequence of ply orientations. The

program was used to minimize coupling stiffnesses that can lead to undesirable behavior under load. Manufacturer-provided ply properties used in the program can be found in Table 2. Poisson's ratio was estimated. A ply orientation of [0/0/90/+45/-45/90/0/0] degrees was chosen, which has the following stiffness matrices:

$$A = \begin{bmatrix} 9.73 & 1.19 & 0 \\ 1.19 & 5.81 & 0 \\ 0 & 0 & 1.38 \end{bmatrix} \cdot 10^7 \text{ N/M} \quad (1)$$

$$B = \begin{bmatrix} 0 & 0 & -6.12 \\ 0 & 0 & -6.12 \\ -6.12 & -6.12 & 0 \end{bmatrix} \cdot 10^2 \text{ N} \quad (2)$$

$$D = \begin{bmatrix} 12.22 & 0.25 & 0 \\ 0.25 & 2.22 & 0 \\ 0 & 0 & 0.41 \end{bmatrix} \text{ NM} \quad (3)$$

Table 2: Ply properties used in computation

Longitudinal Stiffness E_1 (GPa)	Transverse Stiffness E_2 (GPa)	Shear Modulus G_{12} (GPa)	Poisson Ratio ν_{12}
165	8.8	4.3	0.27

It is generally desirable to minimize B_{13} and B_{23}, which couple in-plane stresses with laminate twisting. As these terms are non-zero for this laminate, some warpage may occur during the cure cycle [28]. Perhaps more importantly, the D_{13} and D_{23} terms, which couple bending and twisting, are 0 here. As these braces will be

subjected primarily to out-of-plane loads that may cause bending stresses, it is important that the laminate not twist when subjected to such loads. Extra 0^o plies were added to the outer layers to increase stiffness along the length of the braces. Calculated theoretical longitudinal laminate stiffness (along the length of the braces) is E_x = 94.28 GPa. The two 90^o plies help provide some stiffness in the laminate transverse direction, yielding a calculated theoretical transverse laminate stiffness of E_y = 55.95 GPa. The overall antisymmetric ply orientation was chosen as it can result in a lower stress concentration factor than a crossply laminate (consisting of only 0^o and 90^o plies) [28]. A low stress concentration factor is very desirable, as holes will need to be drilled into the braces to mount hardware.

The prepreg plies must be laid onto a mold with the desired brace shape. Initially, silicone molds (Figure 16) were cast of the orthotic braces used in the CAREX device. However, early composite braces cast from these molds (Figure 16) fit only a few people. Whereas the softer plastic CAREX braces could flex to accommodate larger arms, the composite braces had little flex. To accommodate a wider variety of healthy users (particularly those having soldier body types), new molds were designed in Solidworks. The dimensions were chosen based on a small survey of healthy military-aged males. The molds, seen in Figure 17, also feature flat tops for mounting of the VN-100r sensors. The new molds were milled out of high-temperature epoxy, and designed to create near-net shape braces. As such, 9 mm thick aluminum plates were affixed to the bottom of the molds. These plates allowed excess prepreg to drape better over the edges of the mold, rather than make a nearly 90^o angle at the edge of the mold. Sharp turns near the edges of the molds can lead to poor consolidation of the composite laminate during cure in these areas.

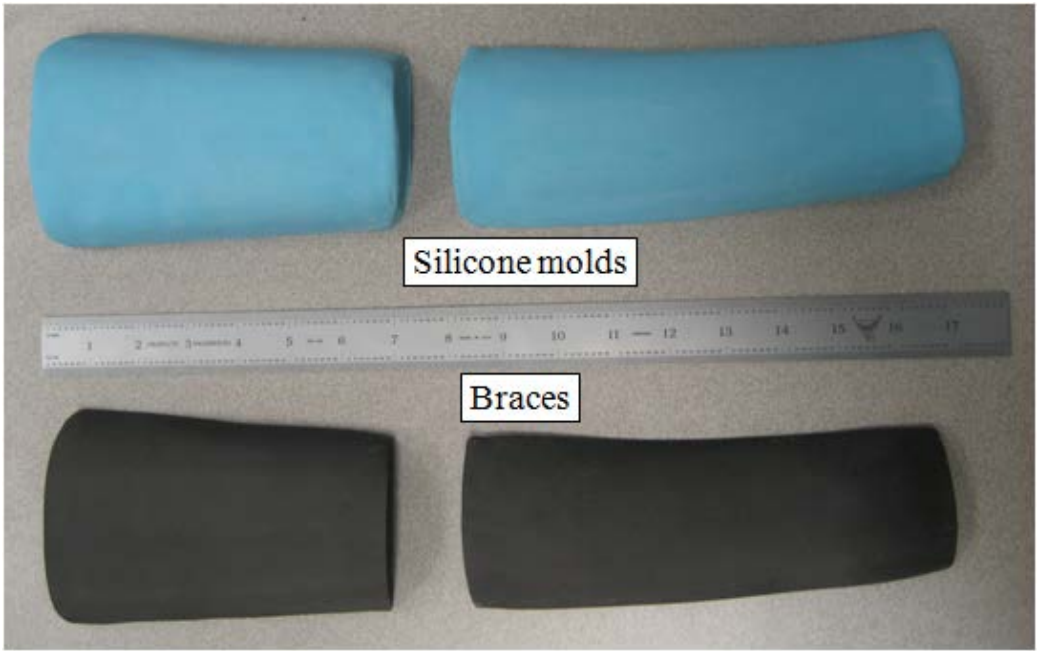

Figure 16: Early silicone molds and braces

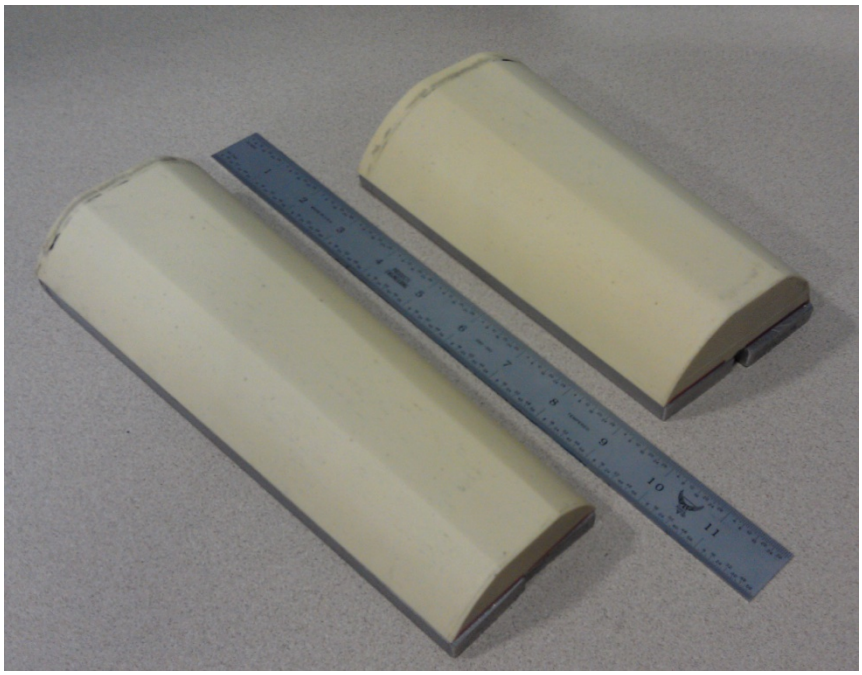

Figure 17: Final molds

The molds were treated with two release compounds: Honey Wax (Specialty Products, Co.) and then Universal Mold Release spray (Smooth-On, Inc.). The molds were then placed on an aluminum caul plate with brown Teflon-coated release sheet (RE234 TFNP50, Airtech International, Inc.) between the molds and plate, as seen in Figure 18. The prepreg plies were laid onto the molds in the afore-mentioned ply sequence. A small aluminum cable termination block, seen in Figure 19, was placed on the upper arm brace after the -45^{o} layer, 25 mm from the distal end of the brace. The remaining 90^{o} and 0^{o} plies were cut slightly to accommodate the protruding cable termination tab. Two 3.1 mm diameter Delrin tubes were affixed to the upper arm brace using small strips of prepreg on the outermost layer of the brace (Figure 20). These tubes were intended to help route the upper arm cables along the braces and provide more protection to the cables. The forearm brace had no integrated cable termination block or routing cables.

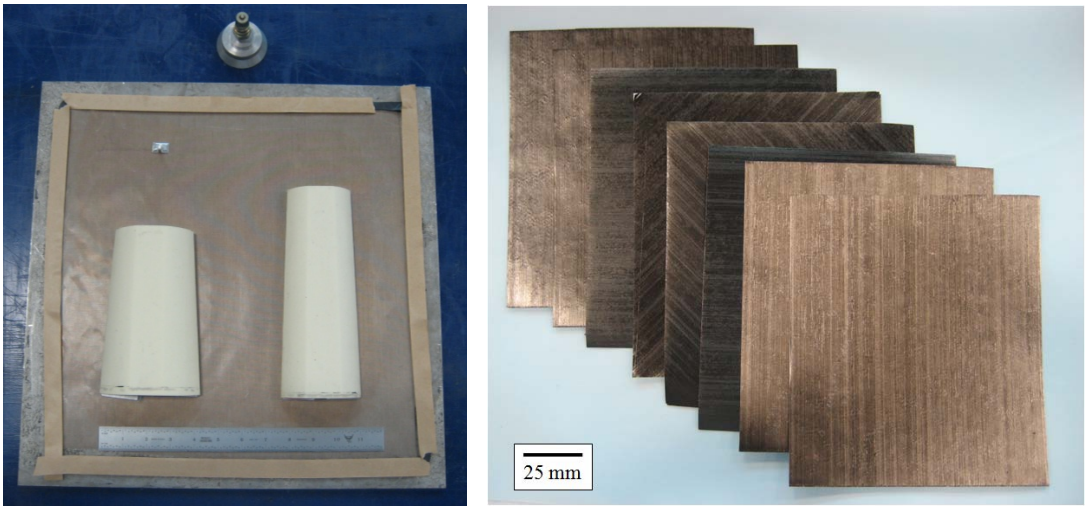

Figure 18: Molds ready for composite lay-up (left), composite plies (right)

Figure 19: Layup process and cable termination block for upper arm mold

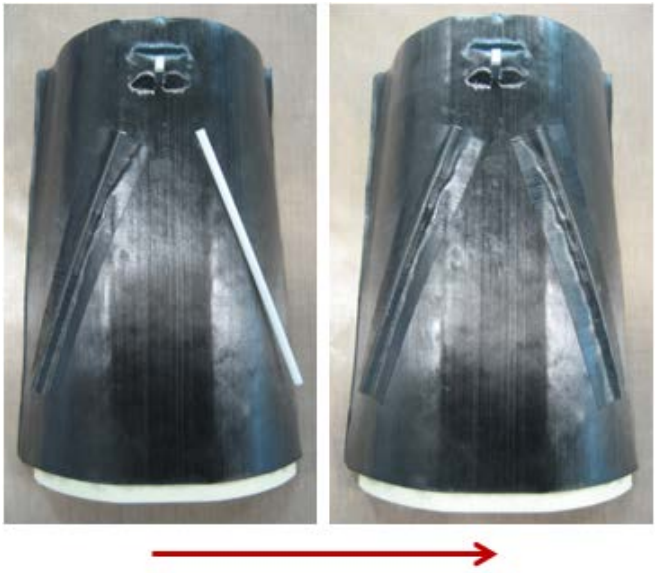

Figure 20: Routing tubes on upper arm mold

Once the prepreg layup process was complete, a blue release ply (1005081 Airtech) was placed over the uncured braces (Figure 21). The release ply was carefully cut near the cable routing tubes and termination blocks. These cuts help avoid wrinkles, which can transfer onto the finished braces, and to help the release ply drape into sharp corners near around the routing tubes. If the release ply bridges over these corners, the cured braces can have incomplete consolidation and dry carbon fibers (without epoxy holding them together) in these areas. A white nylon breather ply (RC-3000-10 Airtech) was then placed over the blue release ply to absorb excess epoxy, and improve pressure distribution and consolidation. Nylon vacuum bag (WN 1500 Airtech) was placed over the white breather ply and sealed with black Tacky Tape (Schnee-Morehead, Inc.).

Figure 21: Vacuum bag process and materials

The braces were then cured per Cytec's specifications for the prepreg: 710 mm Hg vacuum was applied to the layup for approximately 15 minutes. The plate was then placed in a room-temperature oven and temperature was ramped to 127^{o}C (260^{o}F) at 2.8 ^{o}C/min (5^{o}F/min). Temperature was held at 127^{o}C for 100 minutes, then the oven was turned off and the layup allowed to cool down to room temperature gradually over the course of several hours. Vacuum was applied to the layup during the entire ramp-up, hold, and ramp-down cure process. Temperature was monitored using a thermocouple stuck into the Tacky Tape.

After cure, the braces were released from the molds and trimmed to final dimensions of approximately 95×32×160 mm (upper, not including cable mount point) and 75×22×190 (forearm). Holes were drilled in the forearm and outer upper arm braces to attach the VN-100r sensors, cable routing (upper arm brace) and mounting (forearm) brackets. The bracket mounting holes were drilled 12 mm from the edges of the braces and 16 mm apart, as Chou indicated that edge effects in composites extend a distance of 2× of the laminate thickness [28]. After drilling, a 3 mm thick foam (Plastazote) was adhesively bonded to the inside of each brace. The foam is often used in orthoses. Two brackets were then attached to each brace using two brass 8-32 screws per bracket. The use of steel hardware was minimized for weight considerations as well as to avoid interference with the magnetometers in the VN-100r sensors that would be mounted on the braces. The cable routing/mounting brackets were custom designed and cut out of 6 mm thick aluminum plate. They are designed to align the cables that control the forearm with the long axes of the forearm and upper arm, with adjustability to accommodate a variety of arm sizes. A bronze 18 mm long ¼-20 carriage bolt is connected to each forearm mounting bracket using an

aluminum nut. A hole drilled in the end of each bolt provides the termination point for each of the two cables that govern the forearm motion. A 16 mm long piece of ¼-20 threaded Teflon rod with a small lengthwise hole is mounted in each upper arm routing bracket using two aluminum nuts. Each VN-100r sensor was attached to the flat surface of the forearm brace and outer upper arm brace using two 4-40 brass screws and small-profile brass nuts. The braces are attached to the arm using 25 mm wide Velcro straps, which are in turn attached to the braces using adhesive-backed Velcro strips. The completed braces with all hardware and cables can be seen in Figure 22 and Figure 23.

Figure 22: Outer (left) and inner (right) upper arm braces

Figure 23: Forearm brace

3.2.3 Exoskeleton System

The control cables consist of pre-stretched nylon-coated wire rope, approximately 0.9 mm in diameter with a maximum load of 440 N (100 lbs). All six cables are routed through two Teflon blocks on the shoulder cuff, as seen in Figure 24. The shoulder routing blocks are adjustable along the circumference of the shoulder cuff, but remain in place for purposes of this paper. The shoulder cuff is attached to the same frame as the motors, and can be adjusted to each subject's shoulder height. As the shoulder cuff is rigidly attached to a frame, it should help reduce body sway, which has been shown to affect aiming performance [29], [30].

Figure 24: The shoulder cuff and full exoskeleton

Each cable is connected to a Kollmorgen motor. Initially, high-resolution/accuracy AKM43L motors and AKD-P01206 drives were purchased for the project. Unfortunately due to facilities issues, these motors and drives could not be installed. Older Goldline XT motors driven by Kollmorgen ServoStar CD amplifiers in velocity mode were used instead. The motors are mounted on an aluminum frame above the user. Each cable winds onto a 7.24 cm diameter Delrin reel (Figure 25), which is custom designed to prevent the cable from wrapping onto itself. Each cable also passes through a thin rubber sheet to keep it from unwinding from the reel under low tension. A tension sensor (Futek LSB200) with a 220 N (50 lb) limit is mounted in line with each cable between the shoulder cuff and the rubber sheet, as seen in

Figure 25. Care was taken to route the wire for each tension sensor above the sensor, so the weight of the wire does not affect the tension reading. Each tension sensor is paired with and calibrated for an amplifier (Futek CSG100). The tension sensors are attached to the cable with a small plastic clip, which will separate at 90 N (20 lbs) for safety. The Teflon routing points and nylon coating on the cables help reduce friction, as accurate tension sensing is critical to the control of the device.

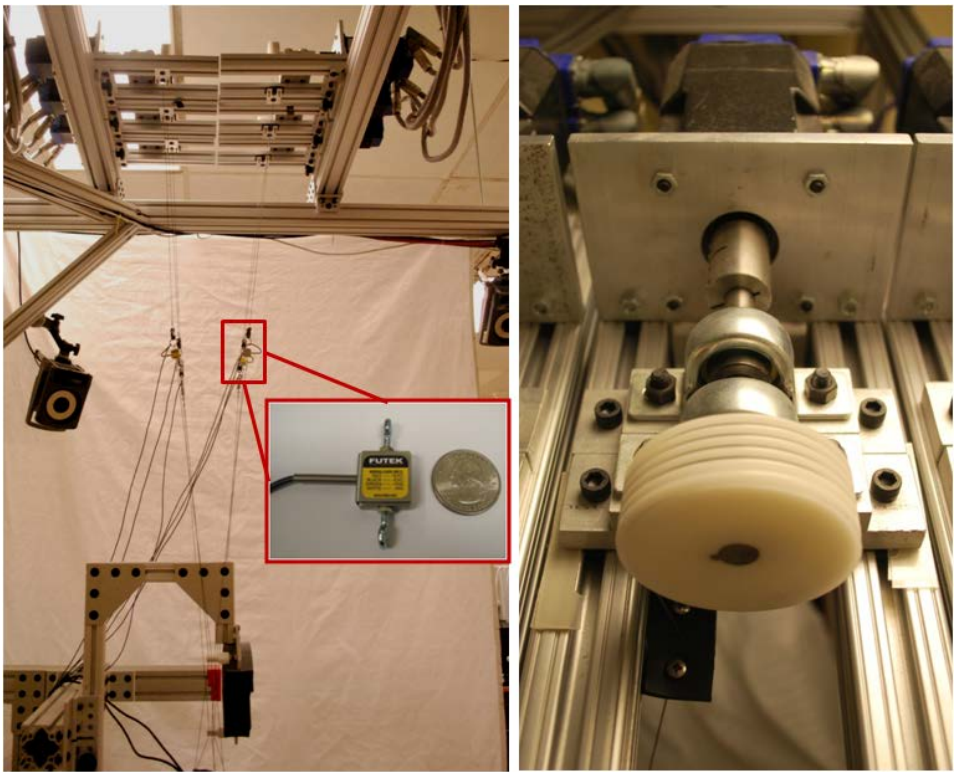

Figure 25: Shoulder cuff, tension sensors, and motors (left), and close-up of a motor and cable reel (right).

The VN-100r gyroscopes are used to directly sense arm tremors and to calculate joint rotation angular rates. The magnetometers are used to calculate joint rotation angles. The IMUs' sample rate is 100 Hz. A National Instruments PXIe

system with FPGA running LabVIEW 2012 is used to interface with the sensors and motors, as well as provide real-time control of the exoskeleton. The real-time control loop runs at 200 Hz on a quad-core PXIe-8133 controller.

3.2.4 Control and Filter: Original Method

MAXFAS is intended only to reduce small tremors while allowing large voluntary movement. However, as the motors are operating in velocity mode, the large voluntary movement of the arm must be explicitly allowed: a zero-volt signal to the motors does not allow any movement. The gyroscopes of the IMUs mounted on the arm braces sense both small tremors and large voluntary movements. Two second-order point-by-point Butterworth filters are employed to separate voluntary and tremorous motion. A 2 Hz cutoff low-pass second-order Butterworth filter isolates voluntary motion to be explicitly allowed by the motors. In parallel, a 4-15 Hz bandpass filter separates the tremorous movement (Figure 26). Previous studies indicate tremors to occur primarily in the 2-15 Hz range, and more specifically the 8-12 Hz range [15], [31]. Movement below 2 Hz is considered voluntary. Early experimentation in MATLAB indicated a lower limit of 4 Hz would provide better cancelling behavior for this system. The isolated 4-15 Hz tremor signal is then sent to a bandlimited multiple Fourier linear combiner (BMFLC). The BMFLC algorithm estimates the tremor signal as a sum of a finite number of sine and cosine signals, with different frequencies within a predefined band $f_h - f_l$. Each sine and cosine is assigned a weight a_r and b_r respectively, which are updated on each loop iteration to reduce error between the estimated tremor signal and the actual tremor signal. The algorithm can be stated as follows (equations 4-7 from [32]). At each time step k, y_k forms an estimate of tremor signal s_k using the equation

$$y_k = \sum_{r=0}^{L} a_r \sin\left(2\pi\left(f_l + \frac{r}{G}\right)k\right) + b_r \cos\left(2\pi\left(f_l + \frac{r}{G}\right)k\right) \tag{4}$$

where $L=(f_h-f_l)G$. For r weights a_r and b_r, equation 1 can be written using reference input vector $\boldsymbol{x}_k$, weight vector $\boldsymbol{w}_k$, and error ϵ_k as

$$x_{rk} = \begin{cases} \sin\left(2\pi\left(f_l + \frac{r-1}{G}\right)k\right), & 1 \le r \le L \\ \cos\left(2\pi\left(f_l + \frac{r-L-1}{G}\right)k\right), & L+1 \le r \le 2L \end{cases} \tag{5}$$

$$\epsilon_k = s_k - \boldsymbol{w}_k^T \boldsymbol{x}_k \tag{6}$$

$$\boldsymbol{w}_{k+1} = \boldsymbol{w}_k + 2\mu \boldsymbol{x}_k \epsilon_k \tag{7}$$

Error ϵ_k is calculated as the difference between signal s_k and the signal estimate. Weights a_r and b_r (in weight vector $\boldsymbol{w}_k$) are updated on each loop iteration (time step) to include the error, reference input vector $\boldsymbol{x}_k$, and adaptive gain μ. Since the tremor estimation signal is comprised of sines and cosines, a prediction of the future tremor signal can be made. In each iteration, the algorithm's main loop calculates the next data point of the tremor signal, negating the amplitude to create a tremor-cancelling signal. An illustration of the algorithm's tremor estimation capability can be seen in Figure 26. The data in Figure 26 was gathered from the VN-100r during the preliminary experiment of Chapter 2. The gyroscope data was processed through the zero-phase filter and BMFLC offline in MATLAB. The result plotted in blue in Figure 26 is the BMFLC prediction of the future tremor at each time step.

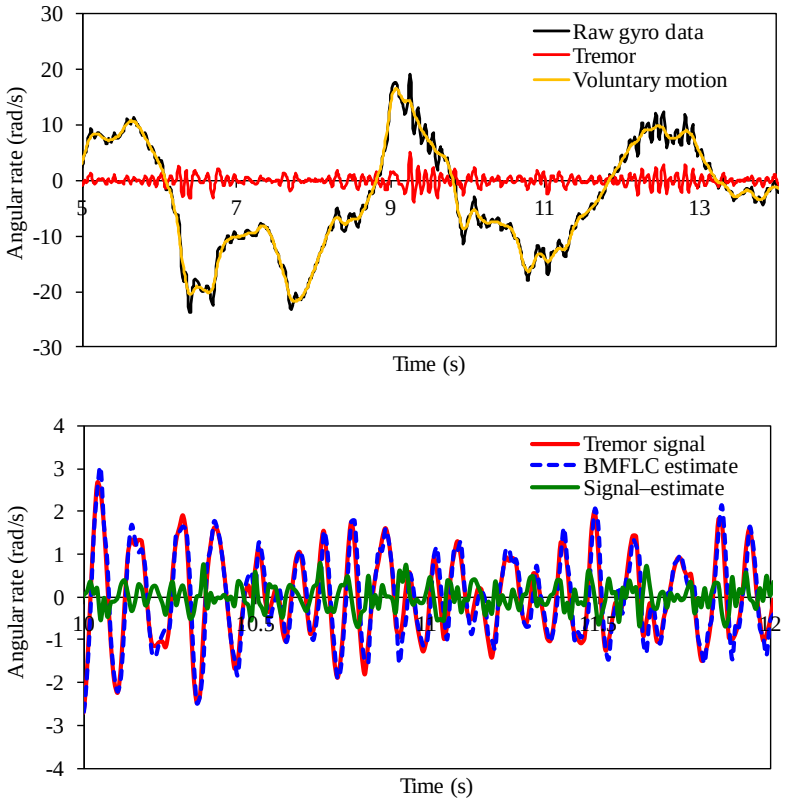

Figure 26: Separation of voluntary and tremorous motion (top), and BMFLC estimate of tremor signal (bottom)

Several variables can be chosen to maximize tremor estimation and thus cancelling. These variables include adaptive gain parameter μ, number of frequency band divisions G, and frequency band $f_h - f_l$. The adaptive gain parameter μ affects the algorithm's ability to estimate the tremor signal, and is inversely related to the algorithm convergence time. A value of $\mu = 0.0825$ was chosen through experiments in MATLAB as a compromise between convergence time and tremor estimation efficacy. Similarly, experimentation in MATLAB revealed G = 5 to provide the best tremor estimation for this system.

The limits of the frequency band can also be expressed using a center frequency f_0, as

$$f_h = f_0 + f_s \tag{8}$$

and

$$f_l = f_0 - f_s \tag{9}$$

Previous research [32] and experimentation in MATLAB indicate 9 Hz as a good initial value for f_0, and f_s = 1 Hz for good tremor estimation. However, in practice, different subjects may have different dominant tremor frequencies ([15], Ch. 2). To accommodate such differences, a fast Fourier transform (FFT) can be used in real-time to measure the exoskeleton wearer's dominant tremor frequency, which then takes the place of the default 9 Hz value for f_0.

In order to calculate joint rotation rates, gyroscope data from the IMUs must be transformed. This transformation involves a least-squares solution for the forearm rotation rates, since $[R_F]$ is a 3×2 rotation matrix in the following equation.

$$[R_U]\cdot\begin{bmatrix}\dot{q}_2\\ \dot{q}_3\\ \dot{q}_4\end{bmatrix}+[R_F]\cdot\begin{bmatrix}\dot{q}_5\\ \dot{q}_6\end{bmatrix}=[R_{s2}]\cdot\begin{bmatrix}\omega_4\\ \omega_5\\ \omega_6\end{bmatrix}, \tag{10}$$

where

$$[R_U]\cdot\begin{bmatrix}\dot{q}_2\\ \dot{q}_3\\ \dot{q}_4\end{bmatrix}=[R_{s1}]\cdot\begin{bmatrix}\omega_1\\ \omega_2\\ \omega_3\end{bmatrix} \tag{11}$$

In Eqs. 10 and 11, $\omega_1 - \omega_3$ and $\omega_4 - \omega_6$ represent gyroscope readings from the VN-100r sensors on the upper arm and forearm, respectively. The terms $[R_U]$, $[R_F]$, $[R_{s2}]$, and $[R_{s1}]$ represent rotation matrices for the upper arm, forearm, forearm sensor, and upper arm sensor, respectively. The terms $\dot{q}_2 - \dot{q}_6$ are the joint angle rotation rates listed in Table 2 below. From Eqs. 10 and 11, it is evident that calculated elbow flexion/extension and forearm pronation/supination rates $\dot{q}_5$ and $\dot{q}_6$, respectively, will be affected by gyroscope signals $\omega_1 - \omega_3$ from the upper arm sensor. Thus, the filter and BMFLC algorithm should be applied to the joint rotation rates after transformation of the gyroscope data. Additionally, the BMFLC can be applied to different joint rotation rates to investigate the effect of cancelling different tremor components. Two scenarios to test different applications of the BMFLC have been programmed into the algorithm, and are listed in Table 3. The general control scheme order can be seen in Figure 27 below.

Table 3: Joint rotation rates

Joint rotation rate	Anatomical movement
$\dot{q}_2$	Upper arm flex/extend
$\dot{q}_3$	Upper arm adduct/abduct
$\dot{q}_4$	Upper arm pronate/supinate
$\dot{q}_5$	Elbow flex/extend
$\dot{q}_6$	Forearm pronate/supinate

Table 4: Test trials

Trial	Condition	BMFLC Filtered signals
1	No MAXFAS	N/A
2	MAXFAS, no control	N/A
3	Filter A	$\dot{q}_3$ $\dot{q}_5$
4	Filter B	$\dot{q}_2$ $\dot{q}_3$ $\dot{q}_5$
5	No MAXFAS	N/A

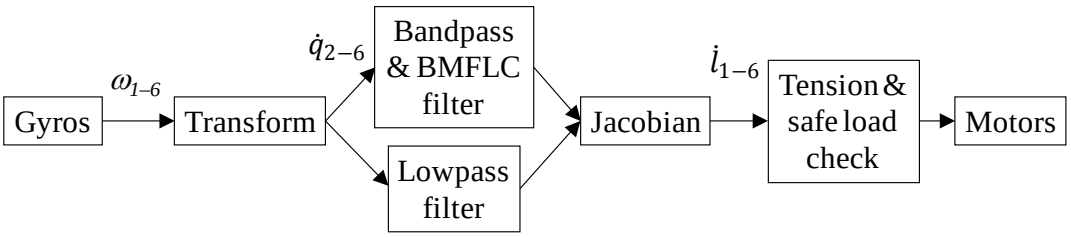

Figure 27: Algorithm flow chart

The terms $\dot{l}_1 - \dot{l}_6$ in Figure 27 are the cable speeds. Once the BMFLC algorithm has built an estimation of the tremor signal, the 4-20 Hz cancelling signal is added to the < 2 Hz voluntary $\dot{q}_{2-6}$ signal. The combined joint rotation rate signals are then transformed to cable speeds using the Jacobian:

$$\{\dot{l}\} = [J]\{\dot{q}\} \tag{7}$$

$$[J] = \frac{\partial l_i}{\partial q_j}, i = 1-6, j = 2-6 \tag{8}$$

The coordinate frames of the arm and the Denavit-Hartenberg parameters used to calculate the Jacobian can be found in Figure 28 and Table 4, respectively. Given the programmed cable speeds, the required motor speeds are calculated using the cable

reel diameter. The cables can only pull, not push, and thus must remain in tension at all times. In order to ensure that the cables are not slack, an algorithm monitors each cable tension sensor. If the cable is taut, the tremor-cancelling motor speed signal is passed from the algorithm to the motors. If the cable is slack, a small constant signal is sent to the motor to wind up the cable. Additionally, the algorithm ensures that the motors do not pull too hard on the arm. If the tension in any cable exceeds 130 N (30 lbs.) for any reason, a small constant signal is sent to the motor to slack the cable.

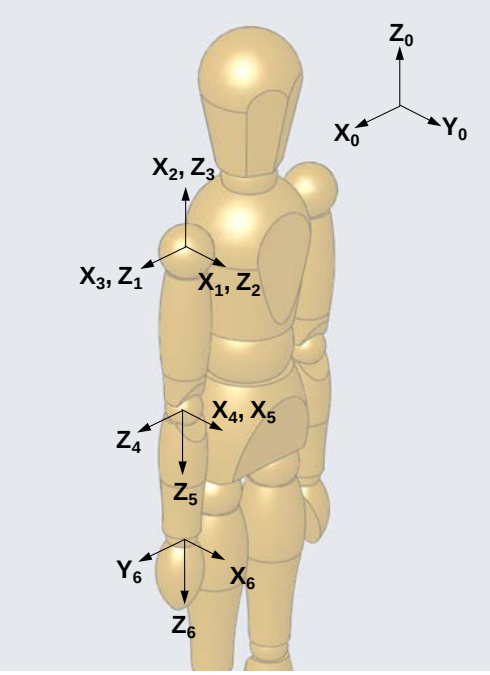

Figure 28: Coordinate frames of the arm

Table 5: Denavit-Hartenberg table for MAXFAS

Link	a_i	α_i	d_i	q_i	Human Joint Motion
1	0	$\pi/2$	0	$\pi/2$	Fictitious joint
2	0	$\pi/2$	0	$q_2 + \pi/2$	Shoulder flexion/extension
3	0	$\pi/2$	0	$q_3 + \pi/2$	Shoulder adduction/abduction
4	0	$\pi/2$	d_4	$q_4 + \pi/2$	Shoulder internal/external rotation
5	0	$\pi/2$	0	q_5	Elbow flexion/extension
6	0	0	d_6	q_6	Forearm pronation/supination

3.2.5 Control: Modified Method

Initial evaluation of the system revealed that the available Goldline XT motors did not have sufficient control bandwidth to produce the tremor-cancelling signals sent by the algorithm. Therefore, the control scheme had to be modified. Two new control scenarios were devised. The first scenario, a 2 Hz cutoff low-pass second-order Butterworth filter operates on gyroscope signals $\omega_1 - \omega_6$ to isolate voluntary motion to be explicitly allowed by the motors. The voluntary motion signals are then transformed into joint rotation rates and cable speeds as described in section 3.2.4 above. Since the cables are only allowing the < 2 Hz large voluntary motion, higher-frequency tremorous motion may be reduced. The second scenario is essentially the same, but adds an “aim check” step. In this scenario, if the standard deviation of the calculated joint rotation rates falls below a minimum value of 0.15 rad/s (over any 0.5 s period), the algorithm sends a 0 volt signal to all of the motors. This signal essentially locks the cables in place, constraining the arm (although not completely). This lock signal is maintained as long as the tension in the cables is at least 18 N (4 lbs), and the standard deviation of the joint rotation rates remains below the specified minimum value. To exit this lock mode and return to normal motion, the wearer

moves their arm slightly to raise the joint rotation rates above the minimum threshold value. The updated algorithm flow chart can be seen in Figure 29, and the updated test trials can be seen in Table 5 below.

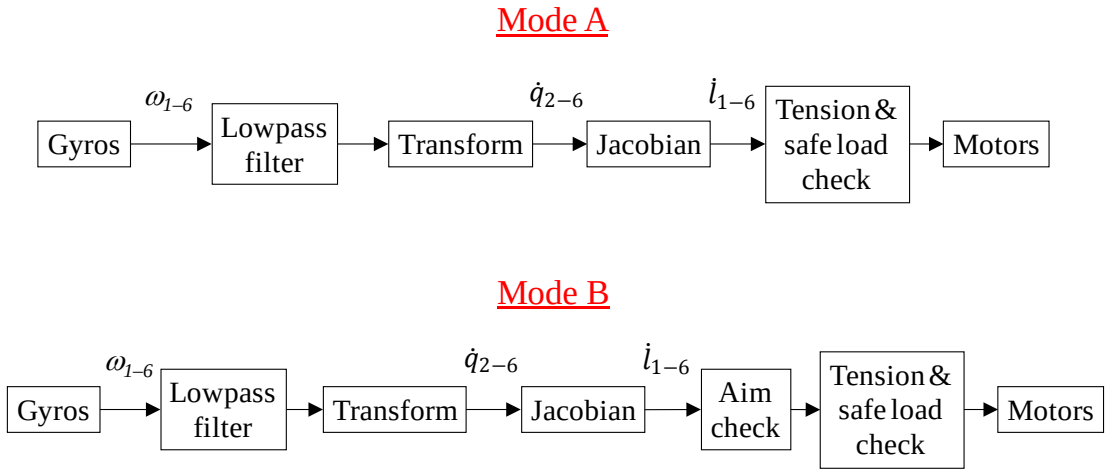

Figure 29: Revised algorithm flow chart

Table 6: Revised test trials

Trial	Condition
1	No MAXFAS
2	MAXFAS, no control
3	Mode A
4	Mode B (lock mode)
5	No MAXFAS

Chapter 4

HUMAN SUBJECTS EXPERIMENTS

4.1 Introduction

This chapter details the system and procedure used to evaluate the effectiveness of MAXFAS on human subjects during a pistol aiming task. Experiments were designed to evaluate the MAXFAS device's effect while wearing the device as well as any learned effects after wearing the device. The MAXFAS device's effects on arm tremor will also be presented and discussed. These experiments are intended to simulate as closely as possible aiming and firing of a real pistol, without the safety concerns associated with firing a real pistol. Use of a simulator pistol greatly simplifies the experiments, allowing them to be performed without eye and ear protection, and in a laboratory rather than at a firing range. Variables associated with firing a real pistol, which are not evaluated in these simulator experiments and may affect live-fire results, will be discussed in section 4.5.

4.2 System

Subjects in these experiments used an airsoft pistol to evaluate aim. The KJWorks M9 PTP was chosen for its similarity in weight and functionality to the Army's standard issue Beretta M9. The M9 PTP uses a CO_2 cylinder to propel an airsoft pellet and recoil the slide. The pistol weighs 1210 g unloaded, including clip, CO_2 gas cylinder, and two rail-mounted lasers (Figure 30). The subject uses a red laser to aim the pistol, while a 780 nm infra-red laser is used by a motion capture system to

track the aim point on the target. The motion capture system consists of 8 Vicon T40-S cameras and a MX Giganet hub. Early experiments revealed that this system can track the laser aim point with sub-millimeter resolution at 100 Hz. The system can also track small reflective spherical markers with the same resolution. Two such markers were placed on the pistol slide (Figure 30) to allow time correlation of each "shot". Here, a shot means that the user pulled the trigger causing recoil but not firing a projectile, as the gun remained empty of projectiles at all times. The shot is counted as the IR laser point on target in the last time frame before the slide began to move backwards in recoil.

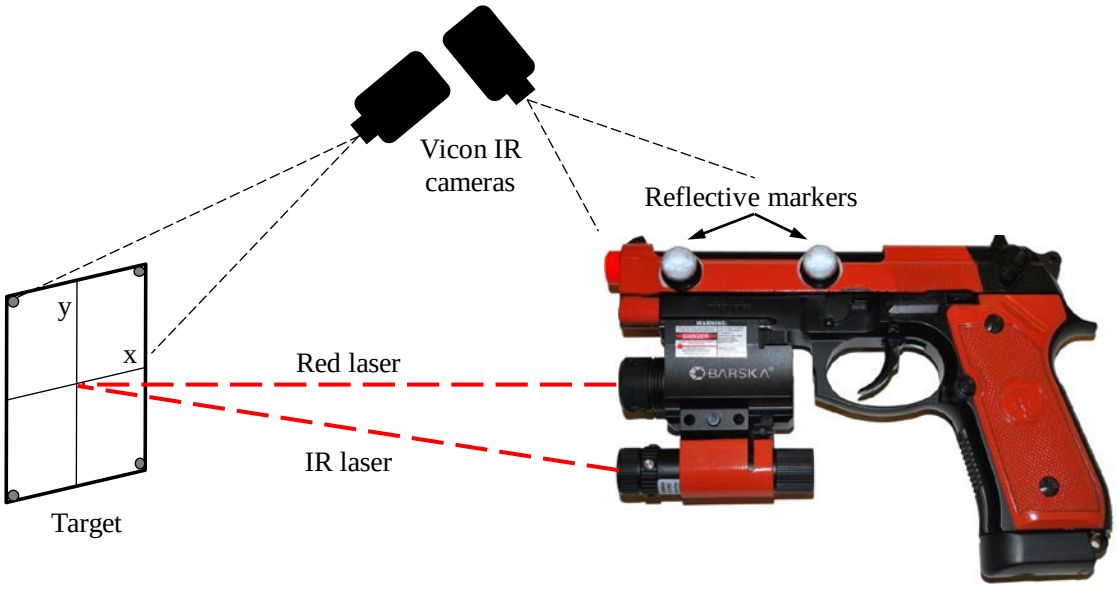

Figure 30: Diagram of aim tracking setup

The target was a white 30×30 cm square with black crosshairs and reflective markers on each corner, seen in Figure 31. The target was mounted with its center 144 cm off the ground, 4 m away from the exoskeleton shoulder cuff. The target is

mounted so that when the subject is standing with their shoulder in the shoulder cuff, the target is essentially centered laterally with the subject. The target was not moved to accommodate geometry differences between subjects.

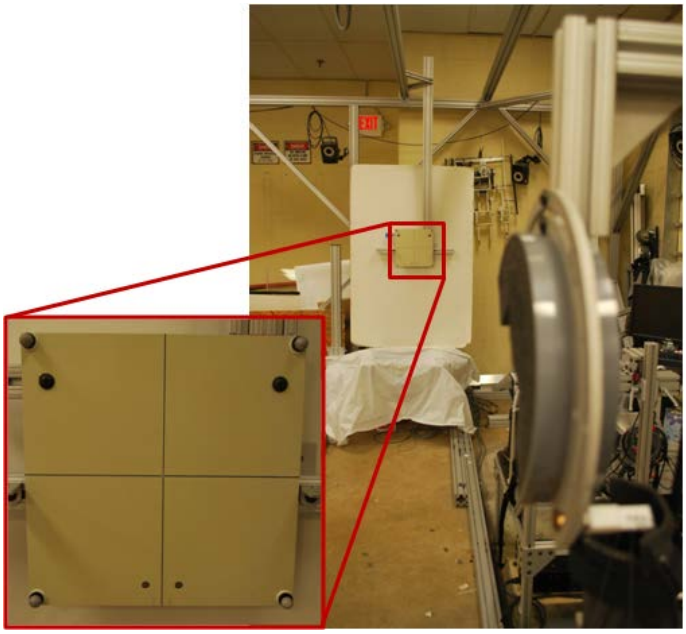

Figure 31: Target mounted 4 m away from shoulder cuff

4.3 Design of Experiments

Twenty right-handed subjects were tested for the purposes of this paper. Fifteen subjects wore the exoskeleton during the experiments and a control group of 5 subjects did not wear the exoskeleton. Before the experiment, each subject read and signed an informed consent form, which can be found in Appendix A. Red and IR laser alignment was verified on the target at range before each subject. The lasers were aligned only with each other, and not the iron sights. Each subject was informed of general operation of the pistol, and instructed to aim with two hands. Subjects were instructed to aim using the red laser only, and not the iron sights of the pistol. Each

subject was then allowed three practice shots to familiarize themselves with the target and operation of the pistol. Since the pistol was unloaded, the slide lock was taped down to keep the pistol from locking open after each shot. All shots were in single action trigger mode. After the three practice shots, each subject performed five trials consisting of 15 shots each. Experimental protocol for the five trials can be seen in Figure 32.

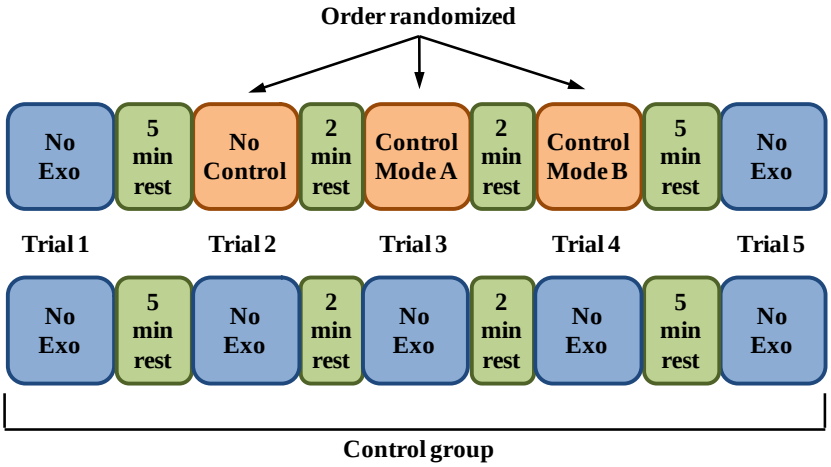

Figure 32: Experimental protocol

In each trial, subjects were instructed when to start and stop, so they did not have to keep track of the number of shots. Subjects were instructed to allow at least 1 s between shots. Early evaluation revealed that a single CO_2 cartridge could provide recoil for up to 80 shots. The CO_2 cartridge was replaced after trial 3 (45 shots) for each subject. Decrease in recoil force was not perceptible after 45 shots. Experimental scenarios are described in section 3.2.5 and Table 5 above. Trial 1 consisted of shooting without the exoskeleton. Subjects then performed 3 trials while wearing the exoskeleton, consisting of two trials with motor control and one trial without motor control. A picture of a subject aiming the pistol while wearing the exoskeleton can be

seen in Figure 32. Experimental scenarios for trials 2-4 were randomized for subjects who wore the exoskeleton, so as to minimize effects of fatigue, learning, and any imperceptible changes in recoil force after replacing the CO_2 cartridge. Finally, subjects performed trial 5, consisting of shooting without the exoskeleton. Subjects in the control group performed all 5 trials using the same timing, but without ever wearing the exoskeleton. All subjects in all trials stood with their shoulder in the shoulder cuff while shooting. Upper arm and forearm length was recorded for each subject, and entered into the Labview algorithm for subjects who wore the exoskeleton. Subject height, age, sex, and shooting experience were also recorded. As caffeine may increase arm tremors [33], subjects were asked to abstain from any sources of caffeine before the experiment. All subjects reported no caffeine intake within a 5 hour period before the experiment.

Figure 33: Subject performing the aiming task while wearing the exoskeleton

The location of the IR laser point on the target was recorded for all subjects throughout each trial. Unfiltered joint rotation rates were also recorded while subjects were wearing the exoskeleton.

4.3.1 Data Analysis

Statistical analysis was performed using SPSS (IBM Corp.). Data were averaged as described below and Friedman's test was used to check for significant differences in each metric among trials. If a metric was found to change significantly among trials, pairwise comparisons were then performed using Wilcoxon signed rank tests. Significant differences described below refer to results of the Wilcoxon tests. Holm-Bonferroni correction was used to control family-wise error rate.

4.4 Results

Average subject age and height for the control group and MAXFAS group (who wore the exoskeleton) can be found in Table 7. Here, "shooters" refers to the number of people in each group who indicated they had some shooting experience.

Table 7: Test group demographics

Group	Average age (years)	Average height (cm)	Females	Shooters
Control	29.8±5.8	173.6±11.4	2	1
MAXFAS	29.1±5.8	176.7±6.7	3	5

Target center location was calculated for each trial using the four reflective markers on the target. Absolute distance from target center (radius R_c) was calculated for each shot. R_c was averaged over the 15 shots in each trial, then averaged across all subjects in each trial. Average R_c of all MAXFAS subjects in each trial can be found in Figure 34. Additionally, each subject's average R_c in trials 2-5 was normalized against their trial 1 R_c (pre-exoskeleton) value. Figure 35 thus presents the average shooting performance for trials 2-5 normalized to each subject's initial performance.

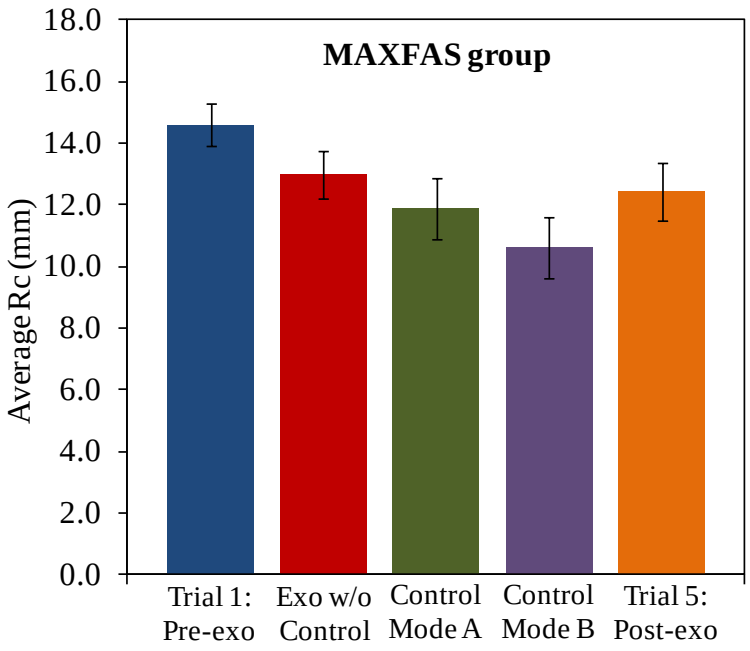

Figure 34: Average distance to target center (R_c) with standard error for MAXFAS subjects

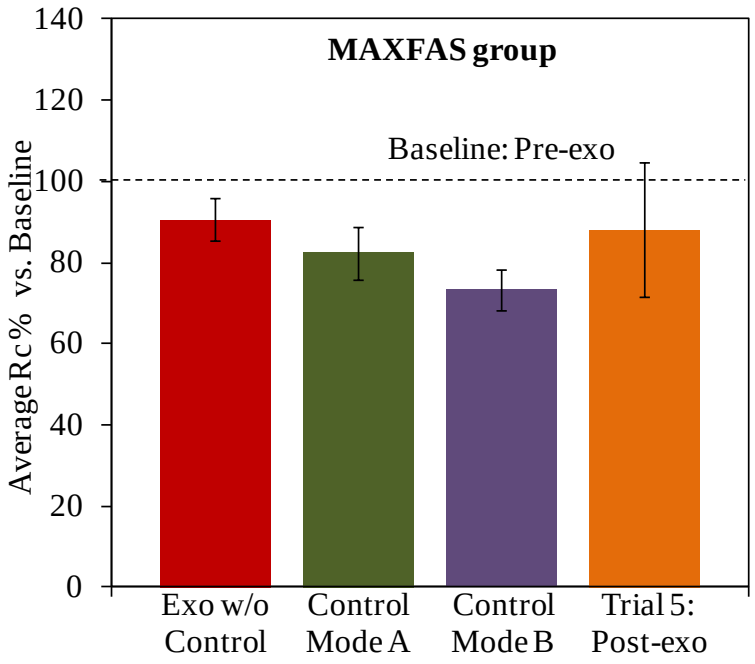

Figure 35: Average R_c for MAXFAS subjects normalized to trial 1, with standard error

Average R_c decreased significantly while subjects wore the exoskeleton using both control mode A and control mode B, compared to trial 1 (pre-exoskeleton). Compared to trial 1, 14 out of 15 subjects had a lower average R_c using control mode B. Average R_c was not significantly lower than trial 1 while subjects wore the braces without motor control. This result indicates that the improvement in shooting performance is not merely attributable to the braces, but that the motor control plays an important role in reducing average R_c. Compared to the trial 1 average, the reduction in average R_c with control mode B was greater and more significant than the reduction in average R_c with control mode A. Additionally, the average R_c for trial 5 (5 minutes after removing the exoskeleton) was somewhat smaller than that of trial 1. Compared to trial 1, 12 out of 15 subjects had a lower average R_c in trial 5. However, this reduction is not statistically significant using the corrected Wilcoxon test

described in section 4.3.1 above. Average R_c of all control subjects in trials 1 and 5 can be seen in Figure 36. The shooting performance of the control group did not improve from trial 1 to trial 5, on average.

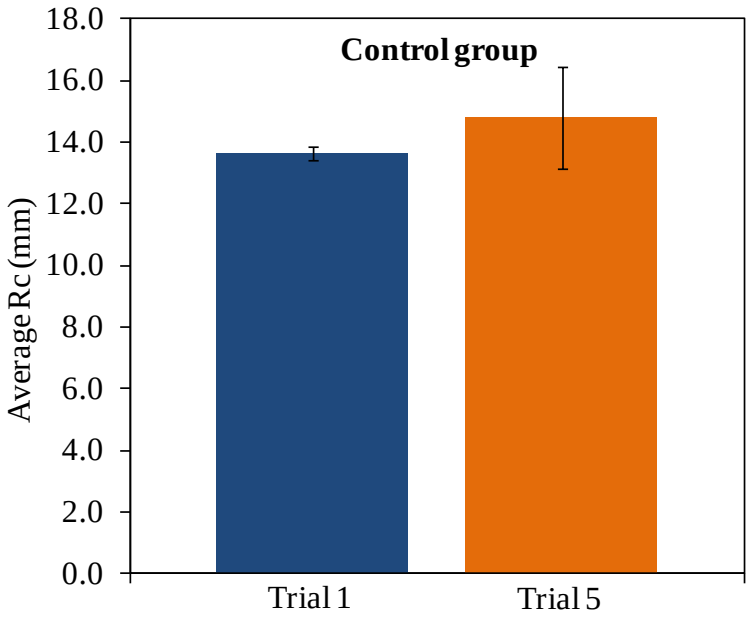

Figure 36: Average R_c with standard error, for control group subjects

Calculated joint rotation rates were analyzed 0.5-1 s before each shot. This short timeframe was chosen to avoid the inclusion of recoil movement for subjects shooting at 1-2 s intervals. Absolute rotation rates were averaged across MAXFAS subjects without and with motor control during this pre-shot time frame. These averaged absolute rotation rates can be seen in Figure 37below. It is apparent that the addition of motor control significantly reduced arm movement in this critical pre-shot timeframe. Also, motor control mode B was more effective at reducing arm tremor

than control mode A. As such, Figure 38 and Figure 39 below will focus on results for control mode B.

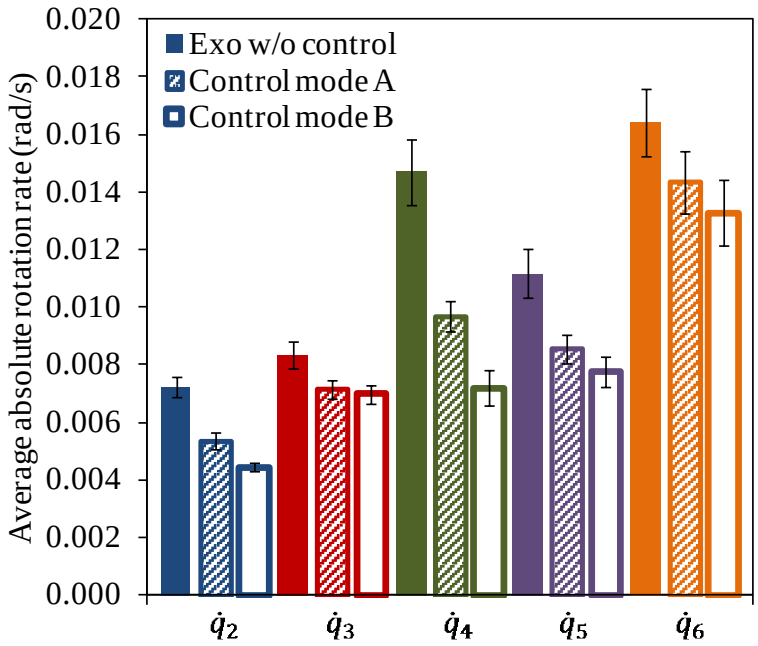

Figure 37: Average absolute rotation rates for MAXFAS subjects without and with motor control (standard error shown)

The fast Fourier transform (FFT) was used on the joint rotation rates to determine the dominant frequency of movement for the same 0.5-1 s pre-shot timeframe as above. The frequency having the maximum amplitude was then averaged across subjects in two scenarios: subjects wearing the exoskeleton with no control, and with control mode B. The results of this FFT analysis can be seen in Figure 38 below.

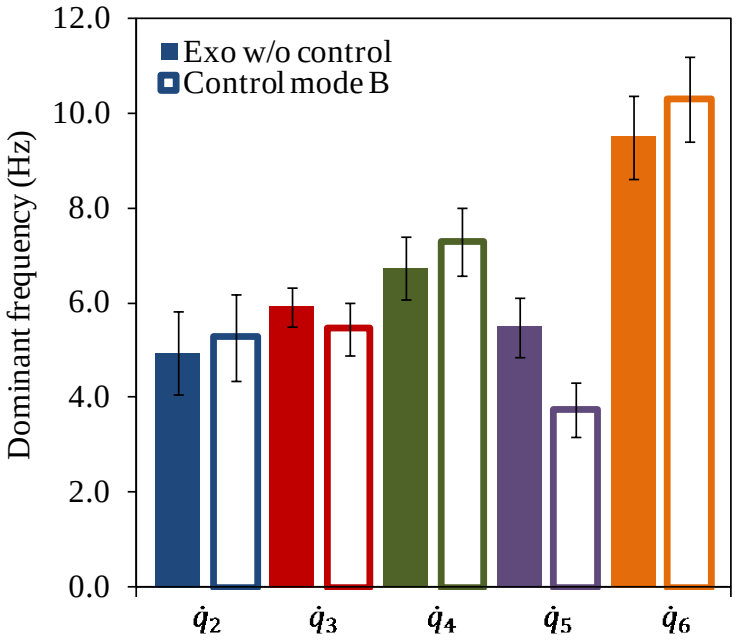

Figure 38: FFT analysis of joint speeds without and with motor control mode B (standard error shown)

Shoulder flexion/extension, adduction/abduction, and internal/external rotation dominant frequencies did not vary much with and without motor control, all staying around 5.9±0.7 Hz. Elbow flexion/extension dominant frequency did change significantly with the addition of motor control mode B, from 5.5±0.6 to 3.7±0.6 Hz. At 9.9±0.9 Hz, forearm rotation dominant frequency did not change significantly with the addition of motor control, but was on average significantly higher than the other measured joint rotation rate frequencies. All numbers given above and in Figure 38 are expressed with standard error.

Absolute laser x- and y-distance from target center was also averaged across MAXFAS subjects in the scenarios mentioned above, as well as trials 1 and 5. These values were measured in the 0.5-1 s before each shot, and the averages are plotted in

Figure 39 below. Average absolute laser x- and y- distance to target center did not change significantly across the trials. However, absolute x-distance to center was significantly smaller than absolute y-distance to target center for all MAXFAS subjects across all trials.

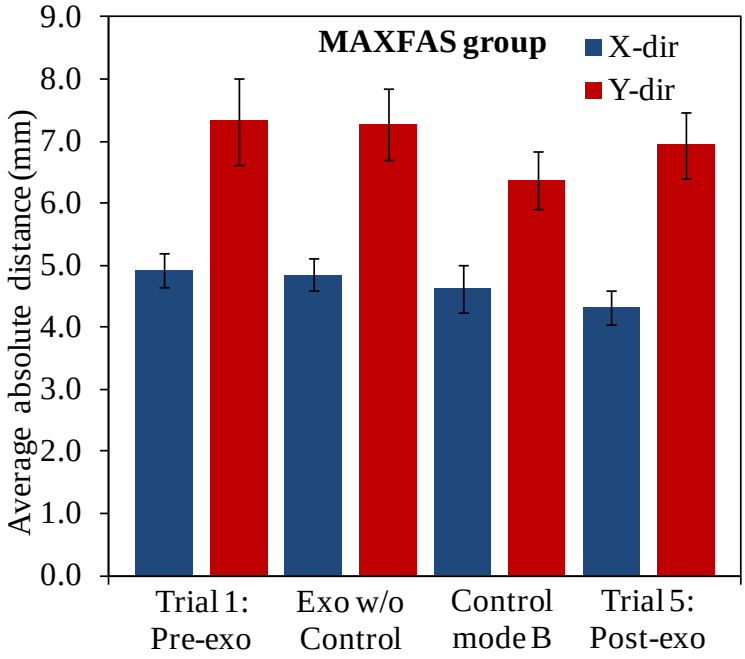

Figure 39: Average absolute laser distance from center for MAXFAS subjects

4.5 Discussion

It is clear that shooting performance improved while subjects wore the exoskeleton. This improvement cannot be attributed to the use of the passive, uncontrolled braces alone. Figure 35 illustrates that the addition of motor control, particularly the “lock mode” of control mode B, significantly improved shooting performance compared to the pre-exoskeleton trial as well as wearing the exoskeleton without motor control. Control mode B resulted in an over 50% reduction in average

R_c for some subjects, compared to the pre-exoskeleton trial 1. These results are very unlikely to be due to "learning" (acclimation to the pistol or task), since the order of trials involving wearing the exoskeleton was randomized. Average shooting performance appeared to be improved 5 minutes after subjects removed the exoskeleton. However, this improvement over trial 1 was slight, and not quite statistically significant using the statistical analysis described in section 4.3.1. However, it should be noted that the control group did not improve on average from trial 1 to trial 5. Indeed, the standard deviation for the control group's average R_c was actually worse in trial 5, which may indicate some fatigue effects. Compared to the MAXFAS group's trial 5 average performance, this result may also indicate that the MAXFAS device may combat fatigue during aiming. It should be noted however that the control group only consisted of 5 people, whereas the MAXFAS group consisted of 15 people.

Figure 37 indicates that a reduction in amplitude of arm shaking coincided with improvement in shooting performance. This reduction was evident in all joint rotation rates, but shoulder flexion/extension, elbow flexion/extension, and curiously, shoulder internal/external rotation were most reduced during the motor control mode B trial. It is expected that a two-hand grip on the pistol will provide more lateral aim stability than vertical stability, and thus the motor control will have less of an effect on shoulder adduction/abduction. Indeed, shoulder adduction/abduction was least reduced by motor control. However, the large reduction in shoulder internal/external rotation using motor control is unexpected. Perhaps this DOF contributes more to aim stability than previously expected.

Figure 39 reinforces the hypothesis that vertical aim stability is weaker than lateral aim stability using a two-handed pistol grip. Y-distance to target was much larger than x-distance to target even with motor control, indicating that further improvements in aim may be achievable by better vertically stabilizing the arm during aim and shooting. Curiously, average x- and y-distance to target changed little with the addition of motor control. Considering that the average R_c and arm tremor (as measured directly by the gyroscopes) were both reduced while wearing the MAXFAS device, the laser average x-and y-distance to target would be expected to be reduced during the 0.5-1 s period before each shot. Why this trend is not borne out in the current results is unclear, but this metric could be investigated in larger future trials in order to verify the expected trend.

Chapter 5

CONCLUSION

This work detailed the scientific challenges of designing, manufacturing, and testing an arm exoskeleton for pistol aim stabilization. The device adds very little weight to the arm, reducing extra arm inertia that cannot be compensated by motors. MAXFAS owes its light weight to a cable-driven architecture, as well as custom-fabricated carbon fiber braces that attach to the arm. These braces were carefully designed and manufactured to provide the necessary stiffness to transmit motor control to the arm while maintaining a very low weight (section 3.2.2). A tremor-cancelling algorithm was designed and optimized for this application (section 3.2.4). While the aforementioned algorithm could not be implemented due to equipment issues, a simpler control method was tested in experiments using human subjects.

Experiments were designed simulate real shooting, using a pistol with recoil, realistic weight and trigger action (section 4.2). Experiments were also designed to eliminate many of the confounding factors involved in aiming and shooting, including body sway, acclimation to the pistol, caffeine intake, and familiarity with iron sights (section 4.3). Experiments were conducted on subjects wearing the MAXFAS device, as well as a small control group who never wore the device. The experiments demonstrated an improvement in shooting performance while subjects wore the device, as well as improved shooting 5 minutes after removing the device. Amplitude of arm shaking, as measured by gyroscopes on the arm, was also reduced while the MAXFAS device's motors applied control to the arm (section 4.4). These experiments

indicated correlation between reduced arm tremors and improved shooting and aiming performance, which is echoed by previous literature.

The implications of this work extend beyond steadying aim. This device could be used to reduce tremor for a number of applications. Those suffering from Parkinson's disease and other debilitating tremors could benefit from active tremor cancelling. MAXFAS could also be used in training for a number of sports and hobbies such as billiards, golf, darts, and archery.

5.1.1 Suggestions for Future Work

This project completed the initial experiments demonstrating that a cable-driven arm exoskeleton could be used to improve pistol shooting performance in a simulated shooting and aiming task. The control mode was limited by the use of outdated motors. First and foremost, the original tremor-cancelling design described in section 3.2.4 should be tested on human subjects using the motors originally purchased for this device. The tremor cancelling algorithm could be combined with the control method demonstrated in this paper, perhaps resulting in further improvement in shooting performance for wearers of the device.

Some slight modifications can be made to the braces based on observations during human subject experiments carried out for this paper. The routing brackets on the upper arm brace should be redesigned to be further away from the arm radially. Extreme care had to be taken while attaching the braces to the upper arm to ensure that these brackets did not pinch the skin of the arm.

The upper arm cables should be routed through the embedded tubes in the upper arm braces. This will require modification of the Jacobian, and may cause excess frictional wear on the cables and Delrin tubes. However, the tubes will likely provide

an optimal path for routing of the upper arm cables and allow for easier attachment and removal of the braces on the upper arm.

The cable that terminates on the bottom of the wrist (ulna side) was observed to occasionally contact the elbow when some subjects bent their elbow. While this contact is not a great concern as most subjects lock their elbows when aiming, this cable should have an extra routing point on the forearm brace to avoid such contact during arm motion from the rest position to the aiming position.

The safety clips attached in line with the load sensors and cables occasionally detached below their 89 N (20 lb) limit. Large aiming movements thus had to be performed slowly to avoid detaching the clips. The clips should be replaced by clips that detach at 133-178 N (30-40 lbs) to allow more natural movement without the fear of prematurely detaching the safety clips. Parameters within the control algorithm could also be modified to allow faster movement.

Finally, experiments should be performed on a larger group of trained soldiers using a real pistol and aiming with the iron sights rather than a laser. Such experiments should also include a large control group. The experiments should involve longer periods of shooting while wearing the exoskeleton, as well as evaluation at later than 5 minutes after removing the device to further evaluate any possible training capability of MAXFAS. Results were good for simulated shooting, but shooting a real pistol using iron sights to aim is very different from the experiments carried out in this work.

BIBLIOGRAPHY

[1] B. J. Makinson, "Research & Development Prototype for Machine Augmentation of Human Strength and Endurance," General Electric Company, Schenectady, NY, 1971.

[2] D. Nosowitz, "Real-Life Iron Man Exoskeleton Gets a Slimmer, More Powerful Sequel," Popular Science, 2010. [Online]. Available: http://www.popsci.com/technology/article/2010-09/real-life-iron-man-suit-gets-sequel. [Accessed 28 2 2013].

[3] Lockheed Martin, "HULC," [Online]. Available: http://www.lockheedmartin.com/us/products/hulc.html. [Accessed 28 2 2013].

[4] Lockheed Martin, "Lockheed Martin's HULC Robotic Exoskeleton Enters Biomechanical Testing at U.S. Army Natick Soldier Systems Center," 2011. [Online]. Available: http://www.lockheedmartin.com/us/news/press-releases/2011/june/LockheedMartinsHULCRoboti.html. [Accessed 28 2 2013].

[5] Raytheon, "Raytheon unveils lighter, faster, stronger second generation exoskeleton robotic suit," PR Newswire, 2010. [Online]. Available: http://multivu.prnewswire.com/mnr/raytheon/46273/. [Accessed 28 2 2013].

[6] S. H. Kim and e. al., "Robot-assisted modifications of gait in healthy individuals," *Esperimental Brain Research,* vol. 202, no. 4, pp. 809-824, 2010.

[7] S. K. Banala, S. H. Kim, S. K. Agrawal and J. P. Scholz, "Robot Assisted Gait Training With Active Leg Exoskeleton (ALEX)," *IEEE Transactions on Neural Systems and Rehabilitation Engineering,* vol. 17, no. 1, pp. 2-8, 2009.

[8] K. N. Winfree, P. Stegall and S. K. Agrawal, "Design of a Minimally Constraining, Passively Supported Gait Training Exoskeleton: ALEX II," in *IEEE International Conference on Rehabilitation Robotics*, Zurich, Switzerland, 2011.

[9] Y. Mao and S. K. Agrawal, "Transition from Mechanical Arm to Human Arm with CAREX: a Cable Driven ARm EXoskeleton (CAREX) for Neural

Rehabilitation," in *IEEE International Conference on Robotics and Automation*, St. Paul, MN, 2012.

[10] J. Klein and e. al., "Biomimetic Orthosis for the Neurorehabilitation of the Elbow and Shoulder (BONES)," in *2nd Biennial IEEE/RAS-EMBS International Conference on Biomedical Robotics and Biomechatronics*, Scottsdale, AZ, 2008.

[11] J. C. Perry, J. Rosen and S. Burns, "Upper-Limb Powered Exoskeleton Design," *IEEE/ASME Transactions on Mechatronics,* vol. 12, no. 4, pp. 408-417, 2007.

[12] P. Letier, M. Avraam, S. Veillerette, M. Horodinca, M. D. Bartolomei, A. Schiele and A. Preumont, "SAM : A 7-DOF Portable Arm Exoskeleton with Local Joint Control," in *IEEE/RSJ International Conference on Intelligent Robots and Systems*, Nice, France, 2008.

[13] S. Balasubramanian, R. Wei, M. Perez, B. Shepard, E. Koeneman, J. Koeneman and J. He, "RUPERT: An Exoskeleton Robot for Assisting Rehabilitation of Arm Functions," in *Virtual Rehabilitation*, Vancouver, Canada, 2008.

[14] G. Wua, F. C. T. v. d. Helm, H. E. J. Veeger, M. Makhsous, P. V. Roy, C. Anglin, J. Nagels, A. R. Karduna, K. McQuade, X. Wangk, F. W. Wernerl and B. Buchholz, "ISB recommendation on definitions of joint coordinate systems of various joints for the reporting of human joint motion—Part II: shoulder, elbow, wrist and hand," *Journal of Biomechanics,* vol. 38, no. 5, pp. 981-992, 2005.

[15] E. Rocon and J. L. Pons, Exoskeletons in Rehabilitation Robotics: Tremor Suppression, Berlin: Springer, 2011.

[16] W. Tang, W. Zhang, C. Huang, M. Young and I. Hwang, "Postural tremor and control of the upper limb in air pistol shooters," *Journal of Sports Sciences,* vol. 24, no. 14, pp. 1579-1587, 2006.

[17] M. Lakie, "The influence of muscle tremor on shooting performance," *Experimental Physiology,* vol. 95, no. 3, pp. 441-450, 2009.

[18] B. Pellegrini and F. Schena, "Characterization of arm-gun movement during air pistol aiming phase," *Journal of Sports Medicine and Physical Fitness,* vol. 45, no. 4, pp. 467-475, 2005.

[19] J. E. Fröberg, C. Karlsson, L. Levi and L. Lidberg, "Circadian Rhythms of

Catecholamine Excretion, Shooting Range Performance and Self-ratings of Fatigue During Sleep Deprivation," *Biological Psychology,* vol. 2, no. 3, pp. 175-188, 1975.

[20] W. J. Tharion, W. R. Santee and R. F. Wallace, "The Influence of Heart Rate, Rectal Temperature and Arm-Hand Steadiness on Rifle Marksmanship During and After Field Marching in MOPP 0 and MOPP I," U.S. Army Research Laboratory, Aberdeen Proving Ground, MD, 1992.

[21] R. S. Goontilleke, E. R. Hoffmann and W. C. Lau, "Pistol Shooting Accuracy as Dependent on Experience, Eyes Being Opened and Available Viewing Time," *Applied Ergonomics,* vol. 40, no. 3, pp. 500-508, 2009.

[22] K. A. Ball, R. J. Best and T. V. Wrigley, "Body Sway, Aim Point fluctuation and Performance in Rifle Shooters: Inter- and Intra-individual Analysis," *Journal of Sports Sciences,* vol. 21, no. 7, pp. 559-566, 2003.

[23] A. A. Ward, H. H. McFann and J. A. Hammes, "A Comparative Test of Accuracy and Speed of Fire with the Improved Loop Sling, with the Combat Rifle Sling and Without a Sling," George Washington University, Alexandria, VA, 1954.

[24] J. Kotovsky and M. J. Rosen, "A Wearable Tremor-suppression Orthosis," *Journal of Rehabilitation Research and Development,* vol. 35, no. 4, pp. 373-387, 1998.

[25] W. D. Hall, "Hand-held gyroscopic device". United States Patent 5058571, 1991.

[26] S. Allen, "Stabilizing device for a gun". United States Patent 5113745, 1992.

[27] Tactical Electronics, "Gyro Stabilized Platform," 2013. [Online]. Available: http://www.tacticalelectronics.com/products/21/products/62/weapon-mounted-cameras/88/gyro-stabilized-platform. [Accessed 28 2 2013].

[28] T. W. Chou, Microstructural Design of Fiber Composites, Cambridge, England: Cambridge University Press, 1992.

[29] K. A. Ball, R. J. Best and T. V. Wrigley, "Body Sway, Aim Point fluctuation and Performance in Rifle Shooters: Inter- and Intra-individual Analysis," *Journal of Sports Sciences,* vol. 21, no. 7, pp. 559-566, 2003.

[30] P. Era, N. Konttinen, P. Mehto, P. Saarela and H. Lyytinen, "Postural Stability and Skilled Performance - A Study on Top-Level and Naive Rifle Shooters," *Journal of Biomechanics,* vol. 29, no. 3, pp. 301-306, 1996.

[31] Y. Mao and S. K. Agrawal, "A Cable Driven Upper Arm Exoskeleton for Upper Extremity Rehabilitation," in *Proceedings of IEEE ICRA*, Shanghai, China, 2011.

[32] K. C. Veluvolu, U. X. Tan, W. T. Latt, C. Y. Shee and W. T. Ang, "Bandlimited Multiple Fourier Linear Combiner for Real-time Tremor Compensation," in *Proceedings of the 29th Annual International Conference of the IEEE EMBS*, Lyon, France, 2007.

Appendix A

INFORMED CONSENT FORM

Study Title: Evaluation of a Wearable Arm Exoskeleton for Aim Improvement of Healthy Individuals

Principal Investigators: **Sunil Agrawal, PhD**
Additional Investigators**:** Dan Baechle

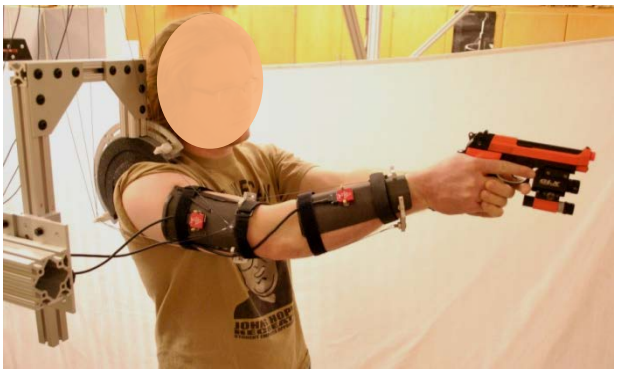

You are invited to participate in a research study for damping of arm movements. You are a healthy adult between the ages of 18 and 40 and will participate in one experiment session at the University of Delaware.

The experiment session will take place in the Mechanical Systems Lab, Spencer Laboratory at the University of Delaware and will take no more than 1 hour.

Participation in this study is voluntary and participants will receive no compensation. You may withdraw from this study at any time without any consequences. If you have severe respiratory problems such as chronic obstructive pulmonary disease (COPD), heart disease, loss of sensation, uncontrolled blood pressure, a seizure disorder, severe arthritis, arm surgery, or other arm orthopedic conditions that limit your activity level, you should not participate in this study. Participants who have upper arm or forearm lengths that are longer or shorter than the exoskeleton will be excluded.

EXPERIMENTAL EVALUATION:

You will aim and “dry-fire” (no ammunition or projectile) a toy pistol 15 times while standing, taking your time to aim between each trigger pull. The toy pistol will be equipped with a red laser to assist your aim at a target approximately 10 feet away. The toy pistol will also be equipped with an invisible laser, which will be tracked by a special camera system in order to evaluate your aim. Next, the exoskeleton will be fitted to your arm. The exoskeleton will apply small forces to your arm while you repeat the aiming/dry-fire task. You will have a brief rest, and repeat the aiming/dry-fire

task again. This will be repeated several times. The exoskeleton will then be removed, and after a brief rest you will repeat the aiming/dry-fire task once more without the exoskeleton. The entire test session should take no more than one hour including setup. The goal is to evaluate any effect on aim that the exoskeleton might have.

RISKS AND BENEFITS:

There is a risk of eye damage if you point the lasers directly at your eye, or anyone else's eyes. Even though the laser power is less than 5 mW, (a standard laser pointer), you should never point the lasers at your eyes or anyone's eyes, as with any laser. *You will only point the lasers at the target, or the ground directly between you and the target. Failure to follow this rule will result in termination of your involvement in the experiment.*

There are slight risks of injury from arm movement with the cable-actuated exoskeleton attached to the arm. These risks include joint and muscle soreness and skin irritation. These risks are minimized in several ways. The motor controller of the device is designed to gently modify the arm movement by applying only small forces. The motors are set to limit the amount of applied force. If forces exceed these values, the motors are automatically shut off. In addition, software defined stops disable the motors when the subject's arm approaches anatomical limits. Both you and the experimenter will have a switch that can be pushed to immediately shut down the motors. Nonetheless, it will be important for you to inform the investigators immediately if you perceive uncomfortable forces being applied to your arm. If you experience any discomfort, the motors will be immediately stopped and appropriate adjustments will be made to reduce the discomfort. Automatic shutoffs and shutdown switches of the exoskeleton will be tested to perform as designed before the experiment.

Pressure from the links of the exoskeleton that modify the arm movement can occur due to faulty alignment, which may result in irritation and redness of the skin. Aligning the braces or the support cuffs for each participant individually reduces these risks. *However, it is important that you inform the investigators if you are experiencing any unusual pressure from the braces or support cuffs while wearing these so that proper adjustments can be made.*

In the event that you are injured or experience acute medical emergency during the study, you will be provided with first aid by the researchers. If you seek or need additional medical care (including care from paramedics), it will be at your own expense.

Your participation may provide valuable information that will help in the design and application of new technology although this may be of no direct benefit to you. This information may help us to improve aim and training for soldiers, competitive shooters, or any other sport or task that requires a steady arm.

STATEMENT OF FINANCIAL INTEREST

Dr. Sunil Agrawal, the Principal Investigator for this study, and other inventors have applied for a U.S. patent protection for the arm device. If the patent is granted, Dr. Agrawal, the team of inventors and the University of Delaware would have a significant financial interest in any commercial development of the device.

CONFIDENTIALITY:

Personal information and the associated case number will be stored in an encrypted and password protected file. Data will be associated directly with the case number alone, not the personal information. Only the researchers will have access to this information. Your individual evaluation results will not be shared with anyone outside the laboratory. Neither your name nor any identifying information will be used in any publication or presentation resulting from this study, unless you provide us consent to use your photographs and/or videos for presentation in seminars and technical papers. The data collected about your aiming performance during these studies will be saved on long-term storage media such as CDs or DVDs, without information that can directly identify you. The media will be stored in the investigator's laboratory in Spencer Laboratory. Following completion of this project, the data will be stored in a secured file cabinet in the investigators' laboratory if the information is deemed to continue to be useful to explore future experimental questions.

Subject's STATEMENT

I have read this consent form and have discussed the procedure described above with the investigator(s). I have been given the opportunity to ask questions, which have been answered to my satisfaction. I understand that any further questions that I might have will be answered verbally, or if I prefer, with a written statement.

In the event that I am injured or experience acute medical emergency during the study, I will be provided with first aid. If I seek additional medical care, it will be at my own expense.

I have been fully informed of the above-described procedure with its possible risks and benefits, and I hereby consent to the procedures. I have received a copy of this consent form.

_____I give permission to use my pictures/videos for presentation in seminars and/or technical papers. (Please initial)

_____ _____

Subject's signature Date

_____.

Subject's Name (please print)

_____ _____

Investigator's Signature Date

If you have any questions concerning your rights as a research participant, you may contact the University of Delaware Human Subjects Review Board (302) 831-2137. Questions regarding the arm exoskeleton, or anything related to the study may be addressed to Dr. Sunil Agrawal (302) 831-8049.

Appendix B

IRB APPROVAL LETTER

UNIVERSITY OF DELAWARE
RESEARCH OFFICE

210 Hullihen Hall
University of Delaware
Newark, Delaware 19716-1551
Ph: 302/831-2136
Fax: 302/831-2828

DATE:	August 31, 2012
TO:	Sunil Agrawal, PhD
FROM:	University of Delaware IRB
STUDY TITLE:	[356678-1] Evaluation of a Wearable Exoskeleton for Aim Improvement of Healthy Individuals
SUBMISSION TYPE:	New Project
ACTION:	APPROVED
APPROVAL DATE:	August 31, 2012
EXPIRATION DATE:	July 17, 2013
REVIEW TYPE:	Full Committee Review

Thank you for your submission of New Project materials for this research study. The University of Delaware IRB has APPROVED your submission. This approval is based on an appropriate risk/benefit ratio and a study design wherein the risks have been minimized. All research must be conducted in accordance with this approved submission.

This submission has received Full Committee Review based on the applicable federal regulation.

Please remember that informed consent is a process beginning with a description of the study and insurance of participant understanding followed by a signed consent form. Informed consent must continue throughout the study via a dialogue between the researcher and research participant. Federal regulations require each participant receive a copy of the signed consent document.

Please note that any revision to previously approved materials must be approved by this office prior to initiation. Please use the appropriate revision forms for this procedure.

All SERIOUS and UNEXPECTED adverse events must be reported to this office. Please use the appropriate adverse event forms for this procedure. All sponsor reporting requirements should also be followed.

Please report all NON-COMPLIANCE issues or COMPLAINTS regarding this study to this office.

Please note that all research records must be retained for a minimum of three years.

Based on the risks, this project requires Continuing Review by this office on an annual basis. Please use the appropriate renewal forms for this procedure.

If you have any questions, please contact Jody-Lynn Berg at (302) 831-1119 or jlberg@udel.edu. Please include your study title and reference number in all correspondence with this office.